Customer	: ESRIN	Document Ref	: SST_CCI-CAR-UKMO-201
Contract No	: 4000109848/13/I-NB	Issue Date	: 09 November 2015
WP No	: 50	Issue	: 1

Project : **SST-CCI-Phase-II**

Title : **ESA SST CCI Phase 2 Climate Assessment Report 1**

Abstract : This document summarises the first climate assessment of the ESA SST CCI Phase 2 Long Term products, Experimental Release version EXP1.2. This includes comparison of the products to other climate data sets of SST. Some user feedback on the Release LT version 1.0 products is also included.

Author :

Chris Atkinson, John Kennedy, Nick Rayner, Met Office Hadley Centre

Anne Stefaniak (registered user of Release LT version 1.0)

Checked :

Ruth Wilson
Space Connexions Ltd

Accepted by ESA :

Craig Donlon
ESA

Distribution : SST_cci team members

Craig Donlon (ESA)

AMENDMENT RECORD

This document shall be amended by releasing a new edition of the document in its entirety. The Amendment Record Sheet below records the history and issue status of this document.

AMENDMENT RECORD SHEET

ISSUE	DATE	REASON FOR CHANGE
Draft A	01 September 2015	First Draft of CAR for review by ESA.
Draft B	04 November 2015	Comments from ESA addressed.
Issue 1	09 November 2015	Document reviewed by SCL.

TABLE OF CONTENTS

1. INTRODUCTION

1.1 Purpose and Scope

This document summarises the first climate assessment of the European Space Agency Sea Surface Temperature Climate Change Initiative (ESA SST CCI) Phase 2 Long Term (LT) products, Experimental Release version EXP1.2. It includes comparison of the products to other climate data sets of SST and some feedback on Release LT version 1.0 products from a user.

PLEASE NOTE: THIS IS AN INTERIM ASSESSMENT OF EXPERIMENTAL RELEASE VERSION EXP1.2. USERS INTERESTED IN A COMPREHENSIVE ASSESSMENT OF THE CURRENT RELEASE VERSION (RELEASE LT VERSION 1.0) SHOULD REFER TO THE CLIMATE ASSESSMENT REPORT PRODUCED IN PHASE 1 OF THE ESA SST CCI [RD.371] (available from http://www.esa-sst-cci.org/PUG/documents).

We assess two EXP1.2 products:

- ATSR. SSTs from Along Track Scanning Radiometer (ATSR) instruments in L3U format at 0.05° latitude by 0.05° longitude resolution covering 1991 – April 2012. (Shortened to SST CCI ATSR.)

- AVHRR. SSTs from Advanced Very High Resolution Radiometer (AVHRR) instruments in L2P format at Global Area Coverage (GAC) resolution covering 1991 – 2013. (Shortened to SST CCI AVHRR.)

The satellite-only SST-depth L4 daily analysis created by the Operational Sea Surface Temperature and sea Ice Analysis (OSTIA) system has not been updated for EXP1.2 and is not discussed here.

1.2 Structure of the Document

After this introduction, the document is divided into a number of major sections that are briefly described below:

Section 2 gives an Executive Summary of the key scientific results, and feedback from one of our users on the Release LT version 1.0 products.

Section 3 presents an assessment of trends and variability in the EXP1.2 products and comparison to other SST products. In order to assess the multi-annual and decadal behaviour of the long-term products, comparisons are made to existing SST data sets including those used by the Intergovernmental Panel on Climate Change (IPCC) in their 5th Assessment Report as well as data sets used in other high profile monitoring reports. Differences between the SST CCI products and the comparison datasets are highlighted. The SST CCI products are also assessed against their Release LT version 1.0 counterparts from Phase 1 of the SST CCI project to determine what progress has been achieved.

Section 4 details the voluntary report received from one of the registered users of the SST CCI Release LT version 1.0 products, describing their application and what they have discovered from using the products.

Section 5 lists any further reported issues identified by the trail blazer users and any other recommendations they have made for future SST CCI products.

1.3 Referenced Documents

The following is a list of documents with a direct bearing on the content of this report. Where referenced in the text, these are identified as RD.n, where 'n' is the number in the list below:

RD.72	Rayner, N.A., P.Brohan, D.E.Parker, C.K.Folland, J.J.Kennedy, M.Vanicek, T.Ansell and S.F.B.Tett 2006: Improved analyses of changes and uncertainties in sea surface temperature measured in situ since the mid-nineteenth century: the HadSST2 data set. Journal of Climate. 19(3) pp. 446-469
RD.74	Rayner, N. A.; Parker, D. E.; Horton, E. B.; Folland, C. K.; Alexander, L. V.; Rowell, D. P.; Kent, E. C.; Kaplan, A. (2003) Global analyses of sea surface temperature, sea ice, and night marine air temperature since the late nineteenth century J. Geophys. Res.Vol. 108, No. D14, 4407 10.1029/2002JD002670
RD.76	Reynolds, Richard W., Thomas M. Smith, Chunying Liu, Dudley B. Chelton, Kenneth S. Casey, Michael G. Schlax, 2007: Daily High-Resolution-Blended Analyses for Sea Surface Temperature. J. Climate, 20, 5473–5496. doi: http://dx.doi.org/10.1175/2007JCLI1824.1
RD.79	Smith, T.M., R.W. Reynolds, Thomas C. Peterson, and Jay Lawrimore, 2008: Improvements to NOAA's Historical Merged Land-Ocean Surface Temperature Analysis (1880-2006). Journal of Climate, 21, 2283-2296.
RD.81	Kaplan, A., et al. (1998), Analyses of global sea surface temperature 1856-1991, Journal of Geophysical Research-Oceans, 103(C9), 18567-18589.
RD.85	Ishii, M., Shouji, A., Sugimoto, S. and Matsumoto, T. (2005), Objective analyses of sea-surface temperature and marine meteorological variables for the 20th century using ICOADS and the Kobe Collection. Int. J. Climatol., 25: 865–879. doi: 10.1002/joc.1169
RD.103	Berry, David I.; Kent, Elizabeth C. 2011 Air–Sea fluxes from ICOADS: the construction of a new gridded dataset with uncertainty estimates. International Journal of Climatology, 31 (7). 987-1001. 10.1002/joc.2059
RD.210	Kennedy J.J., Rayner, N.A., Smith, R.O., Saunby, M. and Parker, D.E. (2011b). Reassessing biases and other uncertainties in sea-surface temperature observations since 1850 part 1: measurement and sampling errors. J. Geophys. Res., 116, D14103, doi:10.1029/2010JD015218
RD.211	Kennedy J.J., Rayner, N.A., Smith, R.O., Saunby, M. and Parker, D.E. (2011c). Reassessing biases and other uncertainties in sea-surface temperature observations since 1850 part 2: biases and homogenisation. J. Geophys. Res., 116, D14104, doi:10.1029/2010JD015220
RD.212	Reynolds, R.W., N.A. Rayner, T.M. Smith, D.C. Stokes, and W. Wang, 2002: An improved in situ and satellite SST analysis for climate. J. Climate, 15, 1609-1625
RD.216	Casey, K.S., T.B. Brandon, P. Cornillon, and R. Evans (2010). "The Past, Present and Future of the AVHRR Pathfinder SST Program", in Oceanography from Space: Revisited, eds. V. Barale, J.F.R. Gower, and L. Alberotanza, Springer. DOI: 10.1007/978-90-481-8681-5_16.
RD.233	Karspeck, A. R., Kaplan, A. and Sain, S. R. (2012), Bayesian modelling and ensemble reconstruction of mid-scale spatial variability in North Atlantic sea-surface temperatures for 1850–2008. Q.J.R. Meteorol. Soc., 138: 234–248. doi: 10.1002/qj.900

RD.239	Roberts-Jones, Jonah, Emma Kathleen Fiedler, Matthew James Martin, 2012: Daily, Global, High-Resolution SST and Sea Ice Reanalysis for 1985–2007 Using the OSTIA System. J. Climate, 25, 6215–6232. doi: http://dx.doi.org/10.1175/JCLI-D-11-00648.1
RD.326	Atkinson, C.P., N.A. Rayner, J. Roberts-Jones, R.O. Smith (2013), Assessing the quality of sea surface temperature observations from drifting buoys and ships on a platform-by-platform basis. Journal of Geophysical Research - Oceans, 118, 3507–3529, doi:10.1002/jgrc.20257.
RD.330	ESA SST CCI Product Validation and Intercomparison Report
RD.332	Woodruff, S.D., S.J. Worley, S.J. Lubker, Z. Ji, J.E. Freeman, D.I. Berry, P. Brohan, E.C. Kent, R.W. Reynolds, S.R. Smith, and C. Wilkinson, 2011: ICOADS Release 2.5: Extensions and enhancements to the surface marine meteorological archive. Int. J. Climatol. (CLIMAR-III Special Issue), 31, 951-967 (doi:10.1002/joc.2103).
RD.334	Rayner, N. A., J. J. Kennedy, R. O. Smith and H. A. Titchner (2013) The Met Office Hadley Centre Sea Ice and Sea Surface Temperature data set, version 2, part 3: the combined analysis. In prep. for JGR Atmospheres
RD.341	Good, S.A., M.J. Martin and N.A. Rayner (2013) EN4: Quality controlled ocean temperature and salinity profiles and monthly objective analyses with uncertainty estimates, Journal of Geophysical Research: Oceans, doi: 10.1002/2013JC009067.
RD.342	Kaplan, A., Y. Kushnir, M. Cane, and M. Blumenthal (1997) Reduced space optimal analysis for historical data sets: 136 years of Atlantic sea surface temperatures, J. Geophys. Res., 102, 27,835– 27,860
RD.343	Lanzante, J.R. (1996), Resistant, Robust and Non-Parametric Techniques for the Analysis of Climate Data: Theory and Examples, Including Applications to Historical Radiosonde Station Data. Int. J. Climatol., 16: 1197–1226. doi: 10.1002/(SICI)1097-0088(199611)16:11<1197::AID-JOC89>3.0.CO;2-L
RD.356	Knight, J.R., R.J. Allan, C.K. Folland, M. Vellinga and M.E. Mann (2005), A signature of persistent natural thermohaline circulation cycles in observed climate, Geophys. Res. Lett., 32, L20708, doi: 10.1029/2005GL024233.
RD.371	SST CCI Climate Assessment Report (CAR), SST_CCI-CAR-UKMO-001, Issue 1, 24 January 2014 http://www.esa-sst-cci.org/sites/default/files/Documents/public/SST_CCI-CAR-UKMO-001-Issue_1-signed-accepted.pdf
RD.373	Dyrrdal, A.V. (2008), A statistical analysis of snow depth variability in Norway and evaluation of Norwegian snow maps. MSc Thesis, North Carolina State University.
RD.374	Deser, C., A.S. Philips and M.A Alexander (2010), Twentieth century tropical sea surface temperature trends revisited, Geophys. Res. Lett., 37, L10701, doi: 10.1029/2010GL043321.
RD.389	Yeo, S.-R., and K.-Y. Kim (2015), Decadal changes in the Southern Hemisphere sea surface temperature in association with El Niño-Southern Oscillation and Southern Annular Mode, Clim. Dyn., doi: 10.1007/s00382-015-2535-z.

1.4   Definitions of Terms

The following terms have been used in this report with the meanings shown.

Term	Definition
AATSR	Advanced Along-Track Scanning Radiometer
AMSR	Advanced Microwave Scanning Radiometer
ATSR	Along-Track Scanning Radiometer
ATSR-1	First ATSR instrument
ATSR-2	Second ATSR instrument
AVHRR	Advanced Very High Resolution Radiometer
CAR	Climate Assessment Report
CCI	Climate Change Initiative
COBE	Centennial in situ Observation-Based Estimates of the variability of SSTs
DMI	Dipole Mode Index
ECMWF	European Centre for Medium-Range Weather Forecasts
EN4	Met Office Hadley Centre dataset
ENSO	El Niño Southern Oscillation
EOF	Empirical Orthogonal Function
ERA-CLIM	ECWMF Reanalysis Archive for Climate
ERSSTv3	Extended Reconstruction SST V3
ESA	European Space Agency
EXP1.2	Experimental Release version EXP1.2 of the ESA SST CCI Phase 2 Long Term products
GAC	Global Area Coverage
HadISST	Hadley Centre Global sea-Ice coverage and SST
HadSST	Hadley Centre Sea Surface Temperature
ICOADS	International Comprehensive Ocean-Atmosphere Data Set
IPCC	Intergovernmental Panel on Climate Change
K	Kelvin
L2P	Level 2 (Pre-processed)
L3U	Level 3 uncollated
L4	Level 4
LT	Long term products
MOHSST	Met Office Historical Sea Surface Temperature data set
NOAA	National Oceanic and Atmospheric Administration (USA)
NOCS	National Oceanographic Centre Southampton
OI	Optimum interpolation
OI.v2	Reynolds et al (2002) Optimal Interpolation analysis

Term	Definition
OSTIA	Ocean Surface Temperature and Ice Analysis
PCA	Principal Component Analysis
PVIR	Product Validation and Inter-comparison Report
RD	Reference Document
RSOI	Reduced Space Optimal Interpolation
RSOS	Reduced Space Optimal Smoother
SST	Sea Surface Temperature
TAMG	Tropical Atlantic Meridional SST Gradient

2.   EXECUTIVE SUMMARY

Here we provide a bullet point summary of the key points from this Climate Assessment Report (CAR).The two ESA SST CCI Experimental Release version EXP1.2 products assessed are:

- ATSR. SSTs from ATSR instruments in L3U format at 0.05° latitude by 0.05° longitude resolution covering 1991 – April 2012. (Hereafter, SST CCI ATSR.)

- AVHRR. SSTs from AVHRR instruments in L2P format at Global Area Coverage (GAC) resolution covering 1991 – 2013. (Hereafter, SST CCI AVHRR.)

These are utilised over the period 1991-2010.

Later in Phase 2, the project will also produce a new satellite-only SST-depth L4 daily analysis created by the OSTIA system from SST CCI ATSR and SST CCI AVHRR products at 0.05° latitude by 0.05° longitude resolution. This has not yet been produced and will be assessed once available.

An aspect of this CAR is that routine comparisons (Section 3) have been automated within the SST CCI system, so that the results can be more easily generated for each future release in a coherent way. This enables the project to be more efficient and cost effective. The purpose of assessing these Experimental Release products is in part as a dry run of more automated approaches to climate assessment (interpretation of automatically generated results is, of course, still required.)

Comparison of SST CCI products to other climate SST data sets and their counterparts from Phase 1 of the SST CCI project (Section 3):

- The SST CCI ATSR and SST CCI AVHRR products are comparable to the main population of comparison data sets in terms of their general evolution of SST and variability.

- The SST CCI AVHRR product has been notably improved relative to the Phase 1 Release LT version 1.0 product in the period prior to 1995, with an anomalous cool bias removed globally and anomalous variability previously seen in some months now reduced.

- The Tropical Atlantic Meridional Gradient and Niño climate indices for the SST CCI AVHRR product are now more consistent with other datasets than was the Phase 1 Release LT version 1.0 product, with spurious spikes and biases no longer evident.

- Spurious variation on annual timescales in the northern Indian Ocean seen in the Phase 1 Release LT version 1.0 SST CCI AVHRR product are no longer evident.

- The SST CCI ATSR product has a discontinuity of order 0.05 K between its ATSR2 and AATSR components as seen in globally averaged SST anomalies. This discontinuity was not seen in the Phase 1 Release LT version 1.0 ATSR product. The AATSR component is warmer than all valid comparison datasets and ~0.05-0.1 K warmer than the Phase 1 AATSR component (which itself is at the upper limit of the comparison ensemble). The reasons for this result are not yet understood.

- Overall trends in SST CCI AVHRR products are inconsistent with those of SST CCI ATSR. In general the SST CCI ATSR product warms faster globally than the comparison data and the SST CCI AVHRR product warms slower globally. Similar, but less pronounced findings were seen for the Phase 1 Release LT

version 1.0 products. For the SST CCI AATSR product this seems partly due to the inhomogeneity between the ATSR2 and AATSR components, whilst for the SST CCI AVHRR product this feature has emerged more clearly now that a cool bias has been reduced in the early part of the record.

- Multi-year variability in the SST CCI ATSR and SSR CCI AVHRR products is generally consistent with that seen in the comparison data.

- Auto-correlations for the SST CCI ATSR and SST CCI AVHRR products are broadly comparable to those seen in other data sets.

Key points arising from use of the SST CCI products by registered users (Section 4):

- The SST CCI data provide useful high-resolution daily data for climate analysis.

- The SST CCI analysis data show clear evidence of multiple climate variability cycles including ENSO. The data compare with additional data sets with some variation. Although further analysis is required, initial results are promising and exhibit many of the trends expected.

Feedback on ease of use of the products (Section 5):

- The L4 data is presented in a standard, easy to access NetCDF data format with a good level of information in the Product User Guide to aid first time users. Some more information regarding the use of the mask would be useful and also the importance of applying the mask.

- Providing the anomaly data would be highly useful and cut down on many individual users' processing time, aiding multi-year comparisons.

- The newly-added SST CCI Easy Download is a great tool for first time users to start using and understanding the data. [N.B. Easy Download is intended only to be used to visually inspect the data, prior to accessing and using products.]

Further recommendations for the future by registered users (Section 5):

- Reprocess the sea ice mask present in the SST CCI analysis, especially for 2008. [N.B., This is in hand, to correct some periods of incorrect persistence of sea ice data.]

- Provide the climatology and/or the anomaly data files (as published in various CCI presentations) to aid analysis and understanding of the dataseets, and information regarding how they have been calculated. For example with the sea level CCI data files both the absolute values and anomalies are available in separate variables within the daily NetCDF files.

- Longer time series of the data sets with more regular updates of recent data particularly with reference to the 2014/15 El Niño would provide highly useful data.

- The tools to extract quick time-series data and subsets of regions would be very useful. The SST CCI Easy Download would be even more useful if you could highlight an area (i.e. draw a rectangle) to download data for a region rather than just one location.

The above recommendations will be taken into the Phase 2 requirements review process, as appropriate.

3. ASSESSMENT OF TRENDS AND VARIABILITY IN SST CCI PRODUCTS AND COMPARISON TO OTHER PRODUCTS

This section assesses the trends and variability in the ESA SST CCI Experimental Release version EXP1.2 products and compares them to other SST products to determine to what extent the new SST CCI products are credible Climate Data Records. The SST CCI products are also assessed against their precursors from the Phase 1 Release LT version 1.0 to determine what progress has been achieved.

This Section makes use of a new automated approach to routine comparison within the SST CCI system, which allows results to be easily generated for each product release in a coherent way. The purpose of assessing the Experimental Release products is in part a first trial of the automated approach to climate assessment. (Interpretation of automatically generated results is, of course, still required). Our expectation is that the final system for producing CAR reports will be as follows: (i) ingestion of the latest SST CCI products; (ii) comparison of the SST CCI products with existing SST datasets and creation of a suite of routine plots and statistics; (iii) display of output on a webpage for the SST CCI team to interpret and comment on; (iv) export of key plots and comments, plus any additional plots marked of interest by the SST CCI team, to a standard CAR document template; (v) manual editing of the standard CAR document to produce the final CAR. Steps (i) to (iv) constitute the automated CAR system (noting that some manual input is required at step (iii)). For this report, steps (iii) and (iv) of the automated system were not available, so the CAR was manually created from the output of step (ii) before circulating amongst the SST CCI team for comment. It is anticipated the full automated system will available for future CARs.

3.1 Introduction

In order to assess the multi-annual and decadal behaviour of the long-term SST CCI products, comparisons are made to existing lower resolution SST data sets. These data sets include those used by the IPCC in their 5th Assessment Report as well as data sets used in other high profile monitoring reports such as the Bulletin of the American Meteorological Society's annual State of the Climate Report. Differences between the SST CCI products and the comparison datasets are highlighted.

3.2 Data sets

The two EXP1.2 products assessed are:

- ATSR. SSTs from ATSR instruments in L3U format at 0.05° latitude by 0.05° longitude resolution covering 1991 – April 2012. (Hereafter, SST CCI ATSR.)

- AVHRR. SSTs from AVHRR instruments in L2P format at Global Area Coverage (GAC) resolution covering 1991 – 2013. (Hereafter, SST CCI AVHRR.)

The project will also produce a new satellite-only SST-depth L4 daily analysis created by the OSTIA system from SST CCI ATSR and SST CCI AVHRR products at 0.05° latitude by 0.05° longitude resolution (hereafter SST CCI analysis). This has not yet been produced and will be assessed once available. For interest, the SST CCI Release LT version 1.0 analysis from Phase 1 is included in the figures in this section.

These are compared to the following data sets over the period 1991-2010.
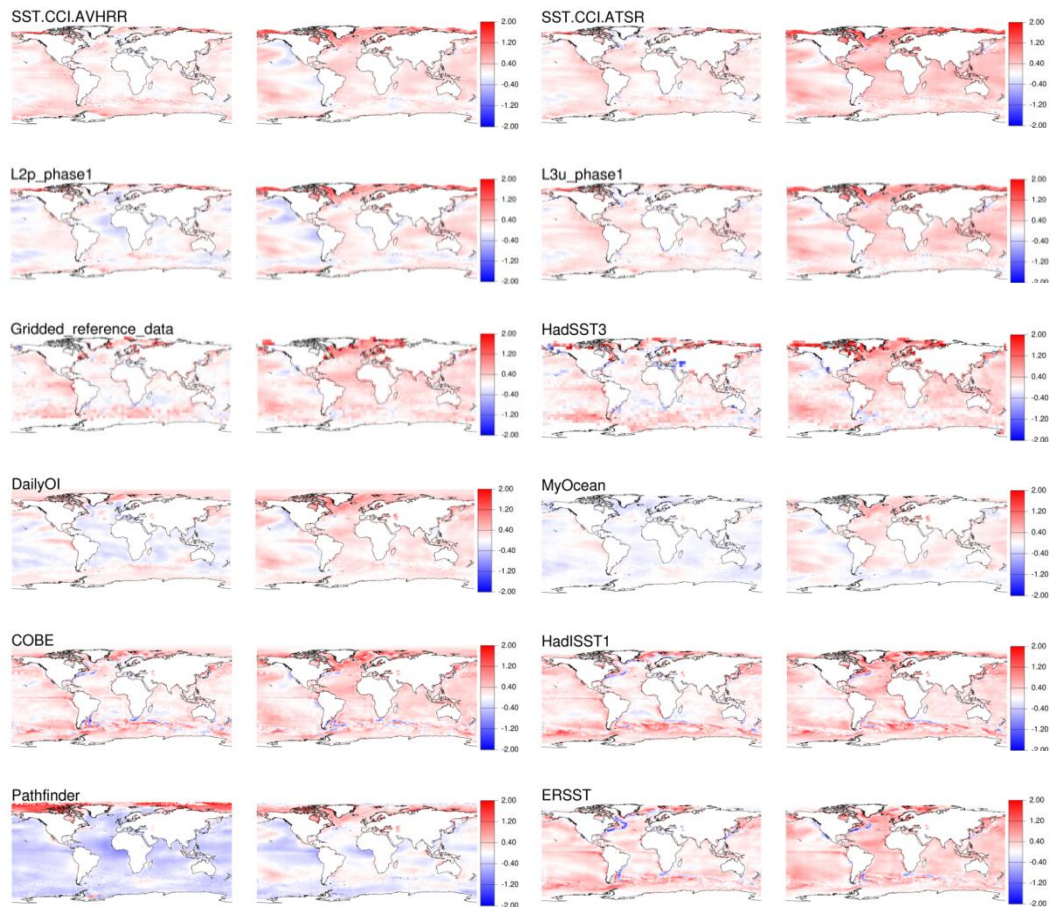
3.2.1   GRIDDED REFERENCE DATA

This data set comprises quality-improved in situ observations from ships and buoys from Atkinson et al. (2013, RD.326) with near-surface observations from Argo profiling floats from EN4 [Good et al (2013), RD.341]. The ship and buoy data are a subset of those used to create HadSST3 (Section 3.2.2). Data from these two sources were averaged onto a regular 5 degree latitude by 5 degree longitude grid at monthly resolution using the method of Rayner et al. (2006, RD.72). The data were not bias adjusted.

This data set will be referred to as the "gridded reference data set" since it comprises information from the reference data set utilised in the PVIR [RD.330, their Section 4.2.4, information reproduced below] together with measurements from ships that have undergone additional quality checking.

The ship and buoy data are a blend of observations taken from ICOADS 2.5 (Woodruff et al., 2011; RD.332) and Met Office Hadley Centre QC flags. The QC flags provided have been produced by the HadISST2 QC system. The general QC procedures are described in Rayner et al. (2006; RD.72) and the high-resolution background climatology and land-sea mask used by this system is described in Rayner et al. (2013; RD.334). This system carries out the following suite of checks: (i) observations are checked for a meaningful location, date and time and that they are not surrounded on all sides by land, (ii) each platform with an individual callsign is tracked to verify its reported position, speed and direction (those without a callsign or with a generic callsign, e.g. SHIP, are passed unchecked), (iii) each SST observation is checked that it is above the freezing point of seawater and within ± 8°C of the 1961-1990 background climatology interpolated to that day, (iv) each SST observations has a "buddy check" applied which compares the value of an individual SST anomaly to the mean anomaly from neighbouring observations; individual observations differing too much from their neighbours are flagged as bad. The HadISST2 QC flags have been supplemented as follows:

1. Drifting buoy SST observations from ICOADS deck 715 have been blacklisted as investigation suggests they are of variable quality. An ICOADS deck identifies the source of the data and refers to the decks of punched cards on which earlier versions of the data set were based. Deck 715 identifies 'German Deep Drifter Data' (originally collected by the Institut für Meereskunde, at the University of Kiel) and provides < 2% of the drifting buoy observations in ICOADS 2.5.

2. Drifting buoy and ship SST observations have an additional QC flag set which follows the procedures described in Atkinson et al. (2013; RD.326). This flag is generated by tracking the quality of observations made by individual drifting buoys and ships over time using the Met Office Operational Sea surface Temperature and sea Ice Analysis (OSTIA) as a reference (a globally complete satellite based analysis). It differs from the SST checks described above in that observation quality is tracked over time to detect biases/instrument failures etc., rather than assessing observations individually. Drifting buoys observations are flagged where they are deemed to be too biased or too noisy, or a buoy is deemed to be out of water having run aground or been picked up. Ship observations are flagged when observations from a particular ship (identified by its callsign) are deemed unreliable (i.e. if a ship callsign is blacklisted all observations from this ship are flagged). In general, ship observations are of variable quality and this flag is intended to reduce ship observations to a higher quality subset; the extra QC excludes between 50 and 60% of ship observations. The development of this extra QC step was funded by the FP7 ERA-CLIM project. This is the first time the information has been used in this way. The benefits of this extra QC are most evident in the assessment of multi-year averages (Section 3.4.2) as persistent poor quality observations from individual buoys and ships can create spurious features of comparable magnitude to true climate variability. For example, in

3. Figure 3-11 the 1991-2000 decadal average anomalies for HadSST3 show a cool streak north east of Hawaii and cool patches in the South Atlantic that are not evident in the Gridded Reference Data or SST CCI products and seem caused by poor quality in situ observations. A preliminary assessment of the benefit of using the drifting buoy QC flags has also been made using the automated PVIR system by repeating the analysis with and without use of all QC flags. In particular, spurious streaks and bull's-eyes are removed from Hovmöller plots of satellite-in situ discrepancies as a function of time and latitude when using the QC flags. Further assessment using the automated PVIR system is planned to drill down to the impacts of particular flags on these results. Finally, it is noted that some further development of these QC flags may be made as part the ERA-CLIM2 project prior to the assessment of the final SST CCI Phase 2 products.

3.2.2   HADSST3

HadSST3 [Kennedy et al. 2011b, RD.210; Kennedy et al. 2011c, RD.211] is an in situ-only data set. Individual observations from International Comprehensive Ocean-Atmosphere (ICOADS) Release 2.5 [Woodruff et al. 2011, RD.332] are averaged onto a 5 degree latitude by 5 degree longitude grid at monthly resolution using the method of Rayner et al. (2006, RD.72). The ship and buoy data used in the gridded reference data set (see above Section 3.2.1) are a subset of the ship and buoy data in HadSST3. Adjustments are applied to the gridded data to account for the effect of systematic errors associated with changes in measurement methods over time. In the period examined here, the principal change is the switch from mostly ship-based observations in the 1980s to a mixture of ship and buoy observations in the late 2000s. Because the exact size of the systematic errors is not known, the data set is presented as an ensemble of 100 different versions (realisations), which are indicative of the uncertainty in the adjustments

applied. Parameters used in the statistical modelling of the biases are varied within their likely ranges to produce an ensemble of bias adjustments. These are then used to create the ensemble of adjusted SST anomaly fields. In addition to the uncertainty associated with the adjustments, there are uncertainties arising from measurement and sampling errors and these are also used.

3.2.3   AVHRR PATHFINDER

The Advanced Very High Resolution Radiometer instruments measure top of atmosphere radiances in the infra red part of the spectrum. AVHRRs have flown on US National Oceanographic and Atmospheric Administration (NOAA) polar orbiting satellites since the early 1980s. The measured radiances can been used to estimate SSTs. This is usually done using coefficients estimated from a regression against drifting buoy or ship data that also vicariously adjusts the AVHRR instrument calibration. Pathfinder v5.2 [Casey et al. 2010, RD.216] is a consistent reprocessing of the AVHRR data from 1981 to 2007. The version used in this analysis was presented on a 1/24 degree equidistant cylindrical grid.

3.2.4   HADISST

Met Office Hadley Centre sea Ice and SST (HadISST) is a globally complete analysis of sea-surface temperature and sea-ice concentrations. It is based on in situ and satellite (AVHRR) measurements of SST. Gaps in the data coverage are filled using a statistical technique known as Reduced Space Optimal Interpolation (Kaplan et al. 1997, RD.342). In areas of the ocean where there is an estimated non-zero sea ice concentration, the SST is inferred from the sea ice concentration. HadISST1.1 [Rayner et al. 2003, RD.74] is presented on a 1 degree latitude by 1 degree longitude monthly grid, although the anomaly analysis is performed on a 2 degree latitude by 2 degree longitude grid (and then added to a 1 degree latitude by longitude climatology) in the modern period (1949 onwards) including the whole period covered in this report.

3.2.5   ERSSTV3B

Extended Reconstruction SST (ERSSTv3b, Smith et al. 2008, RD.79) is another globally complete SST data set. It is based on in situ measurements of SST and uses a combination of Empirical Orthogonal Teleconnections and a low-frequency smoothing to reconstruct SSTs globally. ERSSTv3b is presented on a 2 degree latitude by 2 degree longitude grid. The grid is offset slightly such that the equator passes through the centre of one of the grid boxes rather than forming the boundary of one of the grid boxes.

3.2.6   KAPLAN

The Kaplan data set [Kaplan et al. 1998, RD.81] is a near-globally complete SST data set based on an old version of the Met Office Historical SST data set (MOHSST5). The data are reconstructed using Reduced Space Optimal Smoothing (RSOS). RSOS is similar to RSOI (used in HadISST, Section 3.2.4) and differs in that it uses information about the temporal evolution of SST to reduce the uncertainty in the estimated fields. MOHSST5 has not been update since the late 1990s, so more recent updates have been calculated by processing NOAA SST fields using the same RSOS technique. The data are presented on a 5 degree latitude by 5 degree longitude monthly grid. The data set is not globally complete. Regions of the southern oceans and Arctic ocean – regions where there were too few data to estimate reliable Empirical Orthogonal Functions (EOFs) – are not reconstructed.

3.2.7   COBE SST

The Centennial in situ Observation-Based Estimates of the variability of SSTs (COBE SST, [Ishii et al. 2005, RD.85]) is a globally complete SST data set based on in situ data.

The data are reconstructed using optimal interpolation. In the absence of data the reconstruction relaxes to the climatological average. In marginal ice zones, SSTs are inferred from sea ice concentrations. The data are presented on a 1 degree latitude by 1 degree longitude monthly grid.

3.2.8   NOCS SURFACE FLUX DATA SET V2.0

The National Oceanography Centre, Southampton Surface Flux data set [Berry et al. 2011, RD.103] is based on ship data from ICOADS Release 2.1. The daily data are reconstructed using optimal interpolation. In the absence of data the reconstruction relaxes to the climatological average. The data are presented on a 1 degree latitude by 1 degree longitude daily or monthly grid. The monthly grids were used herein.

3.2.9   KARSPECK ET AL. 2011

Karspeck et al. [2011, RD.233] present an analysis of north Atlantic sea surface temperatures. Their analysis is based on a large scale reconstruction of SST from Kaplan et al. [1998, RD.81] which is then augmented using a mid-scale optimal interpolation. The data set is based largely on in situ data, although satellite data are used to estimate some of the parameters of their reconstruction scheme. The data are presented on a 1 degree latitude by 1 degree longitude monthly grid for the north Atlantic.

3.2.10   OI.V2

The Reynolds et al. [2002, RD.212] weekly and monthly OI.v2 is based on in situ and satellite data. The satellite SST retrievals come from the AVHRR series of instruments and biases in the data are adjusted to more closely match the in situ data. The resulting fields are interpolated using optimal interpolation and the data are presented on a 1 degree latitude by 1 degree longitude weekly and monthly grid. The monthly grids are used herein.

3.2.11   MYOCEAN OSTIA REANALYSIS

The Operational Sea Surface Temperature and Sea Ice Analysis (OSTIA) reanalysis v1.0 [Roberts-Jones et al. 2012, RD.239] from 1985 to 2007 is based on reprocessed satellite and in situ measurements. AVHRR Pathfinder SSTs and retrievals from the ATSR instruments are combined with data from ICOADS Release 2.1 using a multiscale optimal-interpolation scheme. The data are presented on a 0.05 degree latitude by 0.05 degree longitude daily grid.

3.2.12   DAILY OI

Two varieties of the Daily optimum interpolation (OI) version 2 [Reynolds et al. 2007, RD.76] data set were used. One incorporates AVHRR and in situ SSTs and runs from 1981 to present. The other incorporates AVHRR, Advanced Microwave Scanning Radiometer (AMSR-E) and in situ SSTs and runs from 2002 to 2011 covering the period of operation of the AMSR-E instrument. Both varieties use an optimal interpolation scheme to reconstruct missing values and are presented on a 0.25 degree latitude by 0.25 degree longitude daily grid.

3.3   Methods

The SST CCI products and the comparison data sets are presented on a range of different grids and also, in those cases where the data are presented as anomalies, relative to different climatological averages. In order to make a direct comparison, the data were first converted into anomalies relative to the MyOcean OSTIA reanalysis climatology for the period 1985-2007. The climatology was regridded from 0.05-degree

latitude by 0.05-degree longitude daily to have the same resolution as the data set being processed. Secondly, a common mask was applied to the data. Again this was based on the MyOcean OSTIA reanalysis climatology.

3.3.1   LINEAR TRENDS

Time series of area-averaged temperatures were calculated from each of the data sets for the regions shown in Figure 3-1. Area averages were calculated as a weighted average of all non-missing grid box values within the area. The weights were proportional to the area of ocean within the grid box. In coastal grid boxes which were not entirely covered by ocean, the area of ocean was estimated using the OSTIA reanalysis climatology. Grid boxes in the climatology, which had an assigned SST, were assumed to be 100% ocean.

Area averages were calculated for each data set with its native coverage and also after the coverage had been reduced to that of HadSST3. To reduce the coverage to that of HadSST3, each data set first had to be regridded to 5 degree resolution.

Linear trends in the area averages were calculated from all non-missing monthly values using the ordinary least squares method. A resistant method for estimating the trends – median of pairwise slopes [Lanzante 1996, RD.343] - was also used (not shown) to check that outliers did not have a strong effect on the results. Trends were calculated over two periods, 1992-2010 and 1997-2010. The former period covers all complete years in the SST CCI data sets. The latter period excludes the problematic ATSR1/Pinatubo period.
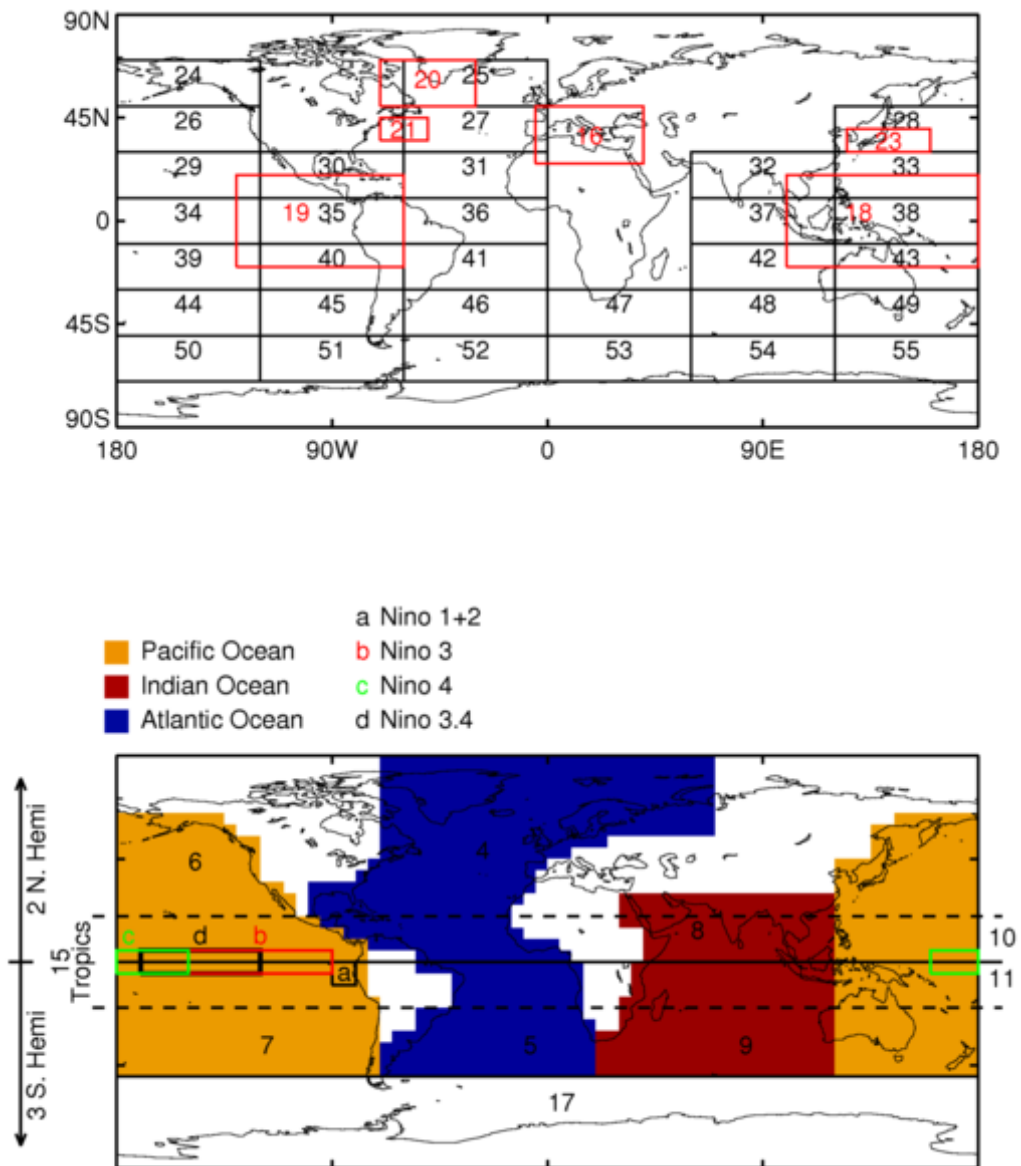
Figure 3-1. Maps showing regions used in the analysis of trends and indices. The regions are also described in Table 3-1.

Table 3-1. List of regions used for the analysis of trends. The regions are shown in Figure 3-1.

Region Name	Region Number	Region Name	Region Number
Globe	1	Area 30°-50°N, 120°-180°E	28
Northern Hemisphere	2	Area 10°-30°N, 180°-120°W	29
Southern Hemisphere	3	Area 10°-30°N, 120°-60°W	30
North Atlantic Ocean	4	Area 10°-30°N, 60°-0°W	31
South Atlantic to 50°S5	5	Area 10°-30°N, 60°-120°E	32
North Pacific Ocean	6	Area 10°-30°N, 120°-180°E	33
South Pacific to 50°S	7	Area 10°N-10°S, 180°-120°W	34
North Indian Ocean	8	Area 10°N-10°S, 120°-60°W	35
South Indian Ocean to 50°S	9	Area 10°N-10°S, 60°-0°W	36
Northern Tropics	10	Area 10°N-10°S, 60°-120°E	37
Southern Tropics	11	Area 10°N-10°S, 120°-180°E	38
Atlantic Ocean to 50°S	12	Area 10°-30°S, 180°-120°W	39
Pacific Ocean to 50°S	13	Area 10°-30°S, 120°-60°W	40
Indian Ocean to 50°S	14	Area 10°-30°S, 60°-0°W	41
Tropics (20°N-20°S)	15	Area 10°-30°S, 60°-120°E	42
Mediterranean	16	Area 10°-30°S, 120°-180°E	43
Southern Ocean, 50°S Southwards	17	Area 30°-50°S, 180°-120°W	44
Western Tropical Pacific	18	Area 30°-50°S, 120°-60°W	45
Eastern Tropical Pacific	19	Area 30°-50°S, 60°-0°W	46
Greenland 50°-70°N, 30°-70°W	20	Area 30°-50°S, 0°-60°E	47
Gulfstream 35°-45°N 50°-70°W	21	Area 30°-50°S, 60°-120°E	48
Southern Hemisphere and Northern Indian Ocean minus rest of NH	22	Area 30°-50°S, 120°-180°E	49
Kuroshio 30°-40°N, 125°-160°E	23	Area 50°-70°S, 180°-120°W	50
Area 50°-70°N, 180-120W	24	Area 50°-70°S, 120°-60°W	51
Area 50°-70°N, 60°-0°W	25	Area 50°-70°S, 60°-0°W	52
Area 30°-50°N, 180°-120°W	26	Area 50°-70°S, 0°-60°E	53
Area 30°-50°N, 60°-0°W	27	Area 50°-70°S, 60°-120°E	54
		Area 50°-70°S, 120°-180°E	55

3.3.2   INDICES

In addition to the time series for the regions described in Figure 3-1 and Table 3-1, indices for certain standard modes of variability were also calculated. These were:

1. Niño 1+2 [0°-10°S, 90°-80°W]

2. Niño 3 [5°N-5°S, 150°W-90°W]

3. Niño 4 [5°N-5°S, 160°E-150°W]

4. Niño 3.4 [5°N-5°S, 170°W-120°W]

5. Dipole Mode Index (DMI) calculated as the difference between the area-average SST anomalies for the regions [50°-70°E, 10°S-10°N] and [90°-110°E, 10°S-10°N]

6. Tropical Atlantic Meridional SST gradient (TAMG) calculated as the difference between the area-average SST anomalies for the regions [60°W-African Coast, 5°-28°N] and [60°W-20°E, 20°S-5°N]

These six indices are all based on area-averages which were calculated in the same way as for the area averages in Section 3.3.1.

3.3.3 MULTI-ANNUAL AND DECADAL AVERAGES

Multi-annual and decadal averages were calculated for the periods 1991-1995, 1996-2000, 2001-2005, 2006-2010, 1991-2000 and 2001-2010. An average was calculated when at least 30% of monthly values were non-missing. In order to highlight multi-annual variability, five-year averages for each data set were also expressed as differences from the 1991-1995 average for that data set. Plots of the decadal-average differences between data sets were also plotted.

3.3.4 AUTOCORRELATIONS

Lagged correlations were calculated for each data set. In order to make a direct comparison, all data sets were re-gridded to 5 degree monthly resolution. Lag correlations at lags of 1, 2, 3 and 4 months were calculated in all grid boxes for which at least 30% of monthly values were non-missing.

3.4 Results

3.4.1 TIME SERIES, LINEAR TRENDS AND INDICES

The SST anomaly time series calculated for this analysis (of which a subset are presented in this section) provide a useful means for assessing the relative biases and evolution of variability in the different data sets considered. In the Phase 1 CAR [RD.371] a comprehensive assessment was made of the same comparison data as used in this assessment. These findings are largely not repeated here as this report focuses on making an interim assessment of experimental release EXP1.2, but the interested reader is referred to the Phase 1 CAR [RD.371]. In general, at global-average scale (Figure 3-2) there are two outliers; NOCS is warmer than the other datasets (the dataset has known limitations in very poorly sampled regions, such as the Southern Ocean) whilst Pathfinder is cooler. The MyOcean OSTIA reanalysis and Daily OI data sets are also cool relative to the other comparison data sets, but the disagreement is not as marked and the variability is similar. In terms of climate variability over the 1991-2010 period of interest, several well-known phenomena are observed in the global-average SST anomalies for most of the datasets (Figure 3-2). In particular: a cooling and subsequent recovery of SSTs over several years following the eruption of Mount Pinatubo in 1991: a sharp warming and subsequent cooling caused by a strong El Niño event in 1997/1998 and successive La Niñas from 1998-2000; and enhanced interannual variability related to a sequence of La Niña–El Niño–La Niña events over the period 2007-2011. In addition there has been a general warming of global SST over this period, as seen in global and hemispheric trends (Figure 3-3).

The upper panel of Figure 3-2 shows the global-average SST anomaly for each of the SST CCI products, the comparison data sets, and the precursor SST CCI products from

Phase 1 of the project. The Karspeck, Kaplan and Daily OI using AMSR comparison datasets are excluded from the time series due to their limited coverage. The SST CCI ATSR and AVHRR products show similar year-to-year variability at a global average scale to that seen in the comparison data sets. There are a few notable exceptions. Between 1991 and 1994 the SST CCI AVHRR product has three pronounced warm spikes. These spikes are seen in time series for both the northern and southern hemisphere but are particularly pronounced in the southern. The global average SST CCI AVHRR product also has some very large warm and cool spikes for a few months in 2010. The exact source of these is difficult to pin down, but investigation of regional time series suggest they may originate in the sub-polar Pacific Ocean, the Arctic and parts of the tropical oceans. The SST CCI ATSR product has pronounced cold and warm spikes in 1996. The cold spike occurs in the northern hemisphere and the warm spike in the southern hemisphere. The regional time series suggest that these originate around the western tropical Pacific and Indonesia, and in the South Atlantic approaching the African coast. A cool spike is also seen in the SST CCI ATSR data in 1997 which seems to originate in the vicinity of Greenland.
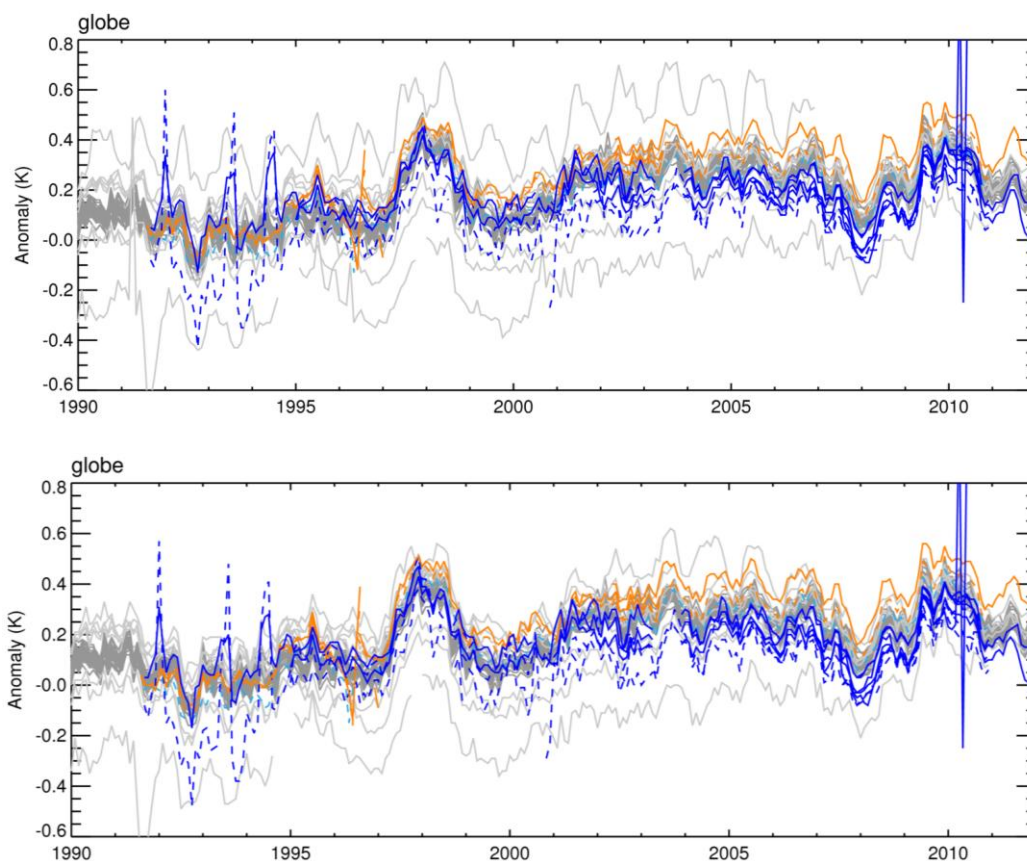
Figure 3-2. Top: Global average SST anomaly (K, relative to MyOcean OSTIA reanalysis climatology) for each of the comparison data sets (grey) and the SST CCI Experimental Release EXP1.2 products [SST CCI ATSR (L3U): orange, SST CCI AVHRR (L2P): blue]. Precursor products from the Phase 1 SST CCI Release LT version 1.0 are shown as dashed lines (these include the Phase 1 SST CCI analysis (L4): green). Bottom: collocated comparison. For SST CCI ATSR and SST CCI AVHRR there is one line for each individual satellite. Kaplan, Karspeck and Daily OI using AMSR comparison data sets are excluded.

Aside from anomalous spikes in the data, the upper panel of Figure 3-2 also highlights some other interesting features of the SST CCI ATSR and AVHRR products. From around 1997 onwards (ignoring the earlier period of anomalous spikes) the ATSR is nearly always warmer than the AVHRR. The offset between them is particularly apparent

for the AATSR period (2002 onwards) and is of order 0.2 K. There is also a notable offset of order 0.05 K between the ATSR2 and AATSR time series for the period when they overlap. During the AATSR period the ATSR data are generally warmer than the comparison data sets and the AVHRR are generally cooler. However, the relative coolness of the SST CCI AVHRR data is much less marked than in the Pathfinder data set, which is also based on AVHRR data.

The global-average SST CCI ATSR and AVHRR data can also be compared with their precursor data sets from Phase 1 of the project. The SST CCI AVHRR dataset compares more favourably to the comparison datasets than its precursor from Phase 1 owing to a general reduction of a relative cool bias. The improvement in the SST CCI AVHRR dataset is particularly pronounced prior to 1995. In this period a large general cool bias has been removed and the magnitude of the anomalous warm spikes has been reduced. Time series for the major ocean basins show that this improvement has been achieved globally in all regions except the Southern Ocean; here the anomalous warm spikes remain present (though a cool bias has been removed). The SST CCI ATSR dataset compares less favourably to the comparison datasets than its precursor from Phase 1 owing to a warmer relative bias for the ATSR2 and particularly AATSR data. Time series for the major ocean basins show that this is especially evident in the northern hemisphere in the Atlantic and Indian Oceans. The reasons for this result are not yet understood. For the ATSR1 data the SST CCI ATSR dataset and its precursor are much more comparable.

Figure 3-3 to Figure 3-6 show linear trends for the SST CCI ATSR and AVHRR products, the different comparison data sets and the precursor products from Phase 1 of the SST CCI project for the various regions are shown in Figure 3-1. Three "outlier" comparison datasets are shown as small grey pips, these are Pathfinder, NOCS and MyOcean OSTIA reanalysis. As for Figure 3-2, the Karspeck, Kaplan and Daily OI using AMSR comparison datasets are excluded. The blue shaded area is an estimate of the measurement and sampling uncertainty as estimated from the HadSST3 data. This indicates the likely spread in trends attributable to weakly-correlated or uncorrelated measurement errors. The spread is generally small for large area averages (e.g. global and hemispheric averages) or for well-sampled regions such as the North Atlantic.

Figure 3-3 and Figure 3-4 show trends for the full 1992-2010 long term record (1991 is excluded because it is partially sampled). Figure 3-5 and Figure 3-6 show trends for 1997-2010 which was chosen because it excludes the problematic ATSR-1 period which includes unusual spikes in the SST CCI ATSR and AVHRR products. Because some of the differences between the SST CCI products and the comparison data sets might arise from differences in large-scale sampling, Figure 3-4 and Figure 3-6 shows the trends over the same period after the coverage has been reduced to that of the *in situ*-only HadSST3 data set. The long-term warming during this period is comparable to the year-to-year variability, which is dominated by the period of high El Niño/La Niña activity around 1997-2000 and again from 2007-2010. Therefore, linear trends are not a good 'model' for temperature change over this period. Nonetheless they do highlight differences such as 'drifts' (or relative instabilities) between the data sets

Figure 3-3 shows that, over the period 1992-2010, in all major ocean basins, the SST CCI ATSR product warms more rapidly than the majority of the comparison data sets, but the SST CCI AVHRR product tends to warm less rapidly. This can be seen in Figure 3-2 for the global average, with the SST CCI ATSR product near the middle or lower end of the comparison data set distribution around 1991 and at the top of the distribution around 2010. These differences persist even after the data sets are reduced to a common coverage (Figure 3-2 lower panel and Figure 3-4) suggesting this is not simply related to changing coverage in the in situ data sets. These differences also hold when a resistant estimator that is less sensitive to outliers is used to calculate the trend (not shown).

Figure 3-3 also shows that the SST CCI product trends are generally less comparable with the comparison datasets in all major ocean basins than their Phase 1 precursors. For the SST CCI AVHRR dataset this finding arises despite the clear improvement in stability of the AVHRR product prior to 1995: the reduction in cool bias for the early-period AVHRR product has not been matched by a warmer product for later AVHRRs, and the effect overall is a reduced trend over time, which is smaller in magnitude than comparators. For the SST CCI ATSR dataset, the less favourable comparison (trends larger than previous products and than most comparators) is likely a result of the jump to warmer values seen between the ATSR2 and AATSR data which was not a feature of the precursor dataset. The effects of this are particularly evident for trends in the North Atlantic and North Indian Ocean regions, consistent with findings discussed earlier.

In terms of the performance of the SST CCI AVHRR and ATSR products, the findings for the 1997-2010 trends (Figure 3-5) are generally similar to those for 1992-2010, though the trends are closer to those of the comparison datasets and sometimes sit within the typical range. Comparing the SST CCI AVHRR dataset to its Phase 1 precursor, the regional agreement with the comparison datasets is more variable for 1997-2010 than was the case for 1992-2010 (which showed generally worsened agreement). In some regions an improved agreement is seen (e.g. the South Pacific and North Indian Ocean regions) while in other regions the agreement worsens (e.g. the North Atlantic and North Pacific Ocean regions). This occurs because the pre-1995 improvement in AVHRR calibration dominates the comparison of 1992-2010 trends but will not affect the comparisons for 1997-2010.
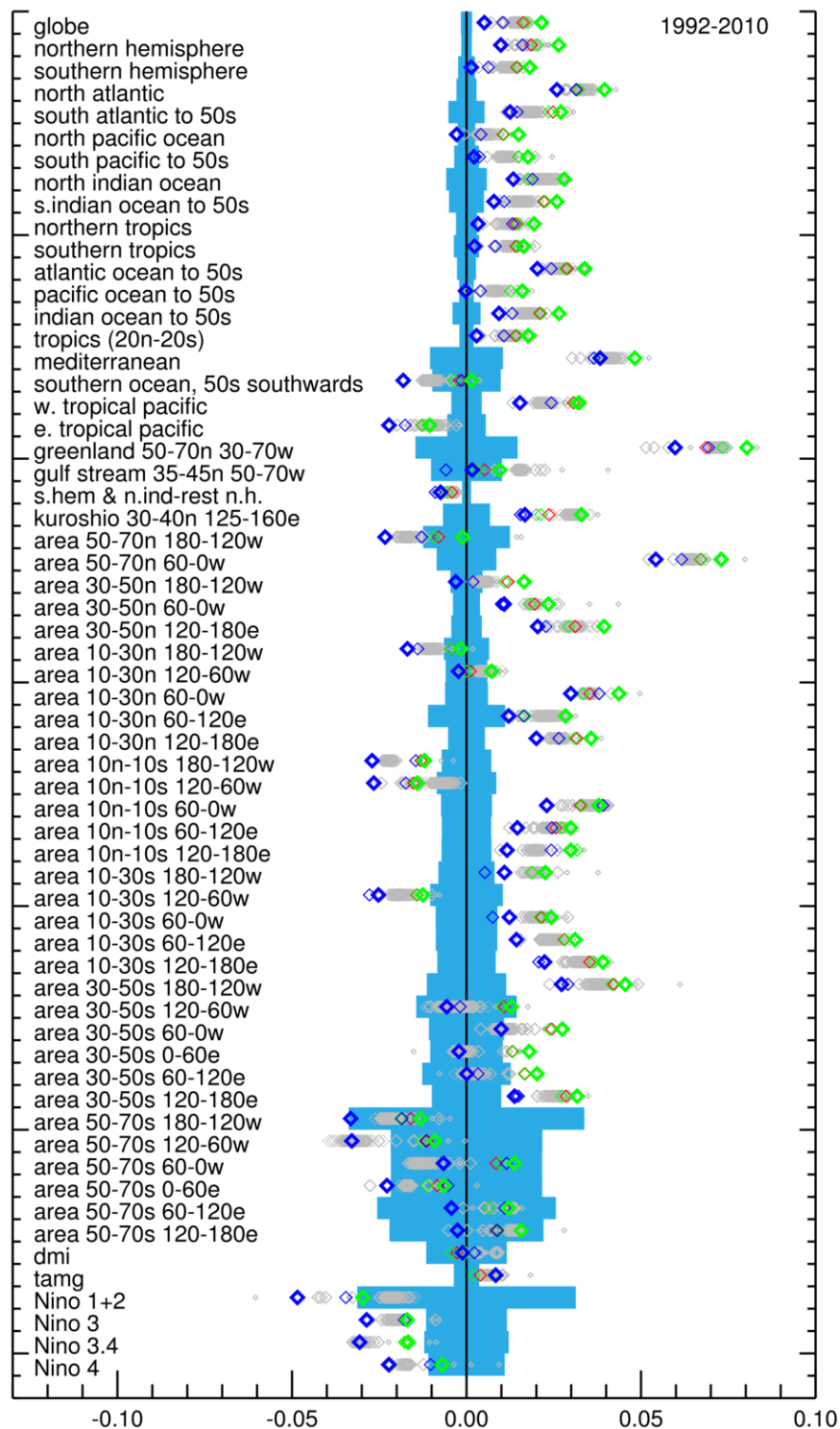
Figure 3-3. Linear trends (K/year) from January 1992 to December 2010 for each of the 61 regions and indices and each of the comparison data sets (grey) and the three CCI data sets: (red) SST CCI Release LT version 1.0 analysis, (green) SST CCI ATSR and (blue) SST CCI AVHRR. The larger green and blue symbols correspond to the Experimental Release EXP1.2 SST CCI products being assessed, and the smaller green, blue and red symbols correspond to precursor SST CCI Release LT version 1.0 datasets from Phase 1. The comparison data sets shown by grey dots are Pathfinder, NOCS and OSTIA reanalysis. Kaplan, Karspeck and Daily OI using AMSR are excluded. The pale blue area is an estimate of the uncertainty in the trend arising from measurement and sampling errors in the HadSST3 data.

Figure 3-4. As for Figure 3-3 but each data set has been reduced to the coverage of HadSST3.
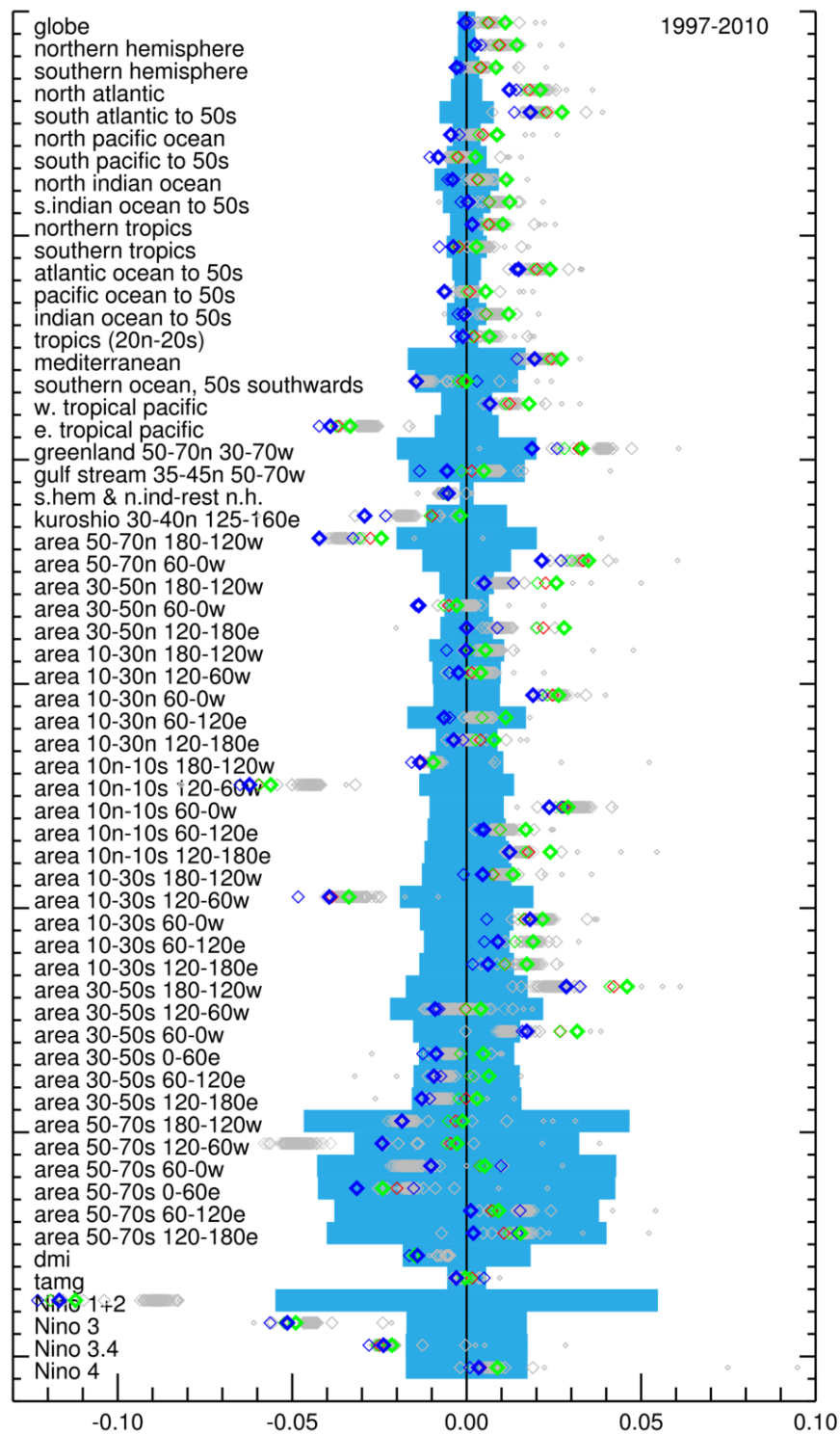
Figure 3-5. Linear trends (K/year) from January 1997 to December 2010 for each of the 61 regions and indices and each of the comparison data sets (grey) and the three CCI data sets: (red) SST CCI Release LT version 1.0 analysis, (green) SST CCI ATSR and (blue) SST CCI AVHRR. The larger green and blue symbols correspond to the Experimental Release EXP1.2 SST CCI products being assessed, and the smaller green, blue and red symbols correspond to precursor SST CCI Release LT version 1.0 datasets from Phase 1. The comparison data sets shown by grey dots are Pathfinder, NOCS and OSTIA reanalysis. Kaplan, Karspeck and Daily OI using AMSR are excluded. The pale blue area is an estimate of the uncertainty in the trend arising from measurement and sampling errors in the HadSST3 data.

Figure 3-6. As for Figure 3-5 but each data set has been reduced to the coverage of HadSST3.

Indices for some standard modes of variability are shown in Figure 3-7 and Figure 3-8. The year-to-year variability in these is largely similar in the SST CCI products to what is seen in the comparison data sets. In Figure 3-7 the spread of estimates is relatively narrow for the Dipole Mode Index (DMI) and the Tropical Atlantic Meridional Gradient (TAMG) because the indices are calculated as the difference between two areas. This tends to reduce the effect of systematic offsets between the datasets. The variability of the DMI and TAMG, and the Niño indices in Figure 3-8, is also much larger than the spread between the datasets.

For the DMI, the strong peak in 1997 and smaller peaks in 1994 and 2006 are larger in the SST CCI products than in most of the comparison data sets. In contrast a peak in late 2009/early 2010 that is seen in most of the comparison data sets is absent in the SST CCI products. This is likely for the same reasons as documented in the Phase 1 CAR [RD.371], i.e. a relative warmth in the western pole of the DMI in those datasets using in situ data for the 2009/2010 peak, and a relative coolness of the eastern pole of the DMI in the SST CCI products for the 1994, 1997 and 2006 peaks (seemingly due to superior feature resolution). Relative to the Phase 1 precursor products the 1994, 1997 and 2006 peaks are smaller, particularly for the SST CCI AVHRR product, while the 2009/2010 peak remains absent in all SST CCI products. These features persist after the data sets are reduced to common coverage.

For the TAMG, the positive peak in 1997 and the negative peak in 2009 are larger in the SST CCI products than in most of the comparison datasets. For the negative 2009 peak, this is likely for the same reasons as documented in the Phase 1 CAR [RD.371], i.e. a relative coolness/warmth in the northern/southern pole of the TAMG that was not as clearly resolved in the comparison datasets. Relative to the Phase 1 precursor products, the SST CCI AVHRR data set seems in better agreement with the comparison datasets, with seemingly anomalous positive and negative spikes removed throughout the period prior to 2004. The SST CCI AVHRR dataset is also now in better agreement with the SST CCI ATSR product than its precursor, notably for the positive peak in 1997 which now has similar magnitude in both products.
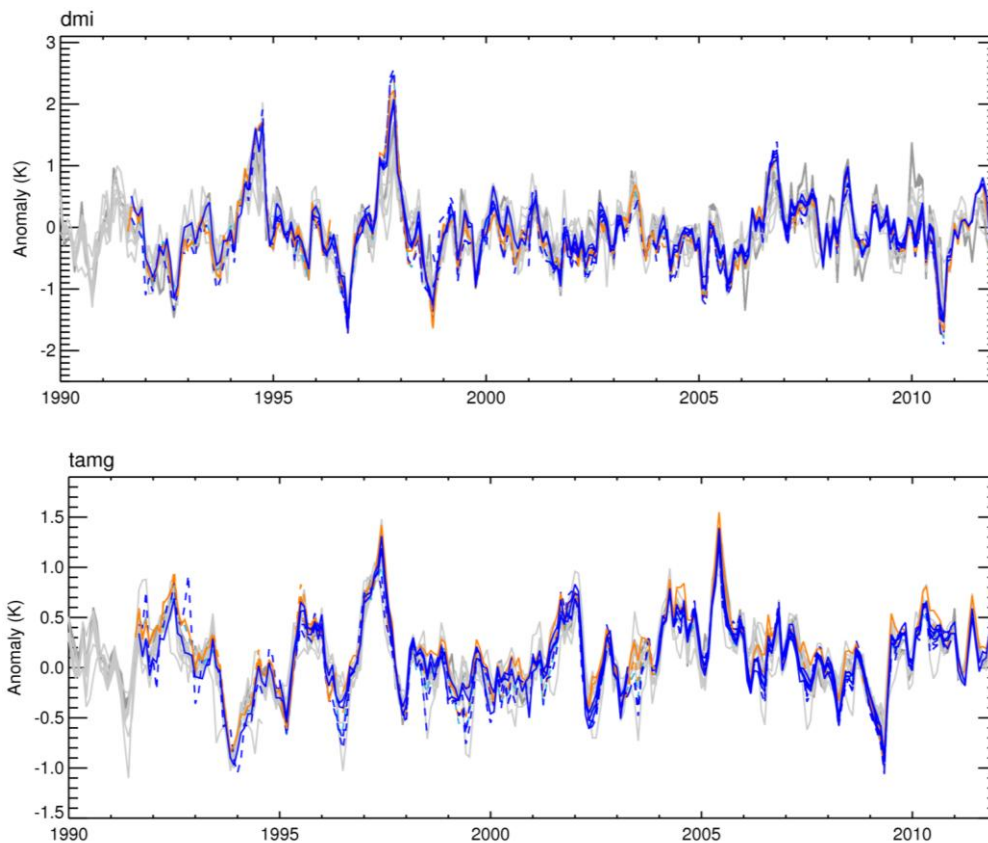
Figure 3-7. Dipole Mode Index (K, top) and Tropical Atlantic Meridional Gradient (K, bottom) for each of the comparison data sets (grey) and the SST CCI Experimental Release EXP1.2 products [SST CCI ATSR (L3U): orange, SST CCI AVHRR (L2P): blue]. Precursor products from the Phase 1 SST CCI Release LT version 1.0 are shown as dashed lines (these include the Phase 1 SST CCI analysis (L4): green). Units are in K because the indices are calculated as the difference between two simple area averages of temperature.

For the Niño regions, all data sets resolve the strong year-to-year variability associated with ENSO. Relative to their precursor datasets two features stand out. For the SST CCI ATSR product, some anomalous spikes are now seen in the Niño 1+2 and Niño 3 regions in 1997. For the SST CCI AVHRR product a cool bias has been removed which was most conspicuous prior to 1995 and in the Niño 1+2 region. This has reduced the 1992-2010 trends for the SST CCI AVHRR product in the Niño indices regions such that the trends are now generally lower than the comparison datasets (Figure 3-3). In the Niño 4 region some anomalous variability prior to 1995 has also been removed from the SST CCI AVHRR product.

Some interesting features are also seen in some of the other regions. In region 8, the North Indian Ocean, the precursor SST CCI AVHRR product had a spurious annual cycle, with periodic cool 'dips', relative to the other data sets (Figure 3-9). This was also seen in region 32 (which is a subset of region 8). In the latest SST CCI AVHRR product this behaviour is no longer as evident. Region 31 also showed some evidence of spurious variability, which is no longer as evident in the latest SST CCI AVHRR product (Figure 3-9). Both these regions are subject to intermittent desert dust, and this suggests that EXP1.2 products are less adversely affected during these episodes than the Phase 1 products.
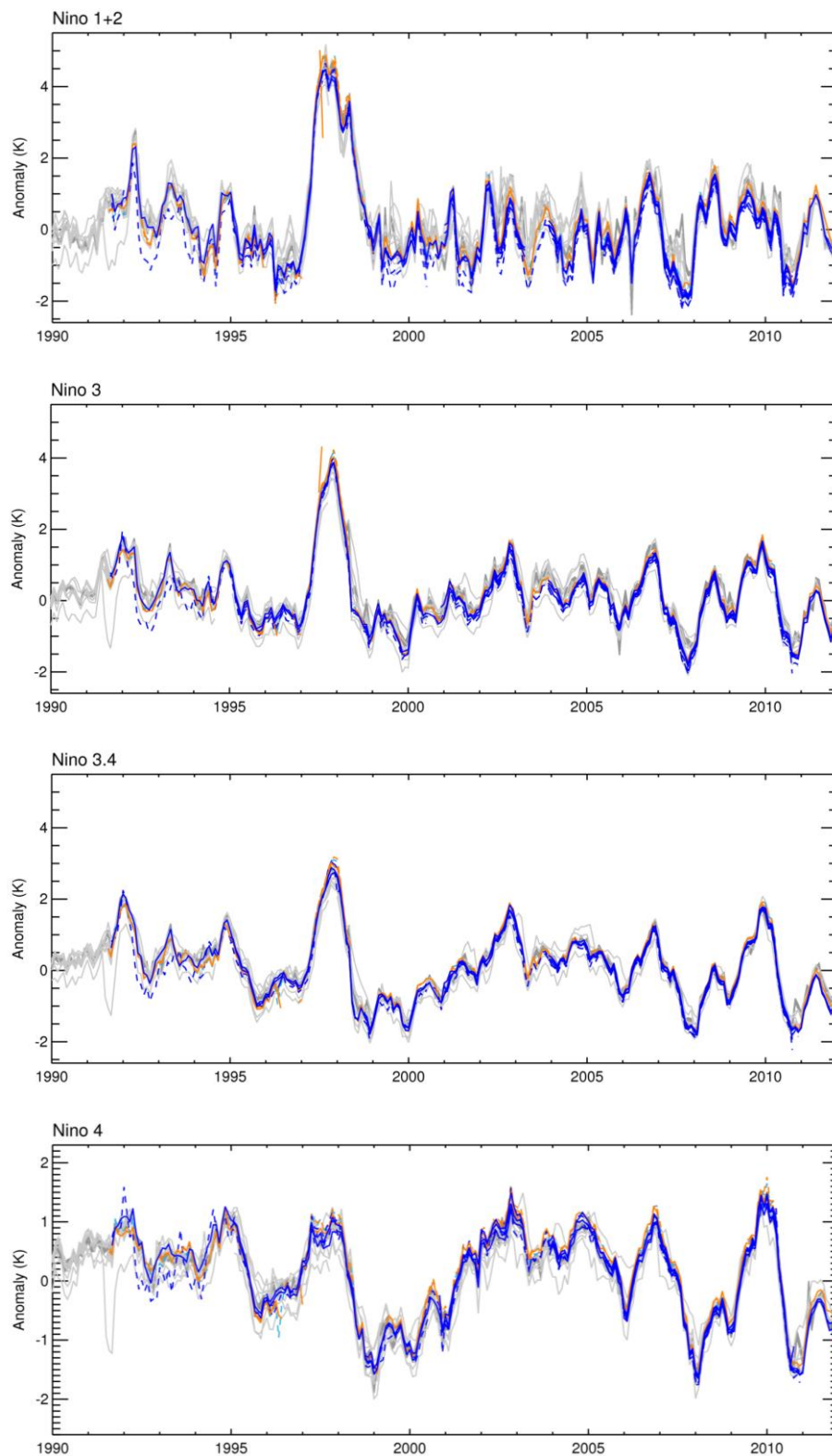
Figure 3-8. Niño indices. Area-average SST anomalies (K) for the four Niño regions described in Figure 3-1 for each of the comparison data sets (grey) and the SST CCI Experimental Release EXP1.2 products [SST CCI ATSR (L3U): orange, SST CCI AVHRR (L2P): blue]. Precursor products from the Phase 1 SST CCI Release LT version 1.0 are shown as dashed lines (these include the Phase 1 SST CCI analysis (L4): green).
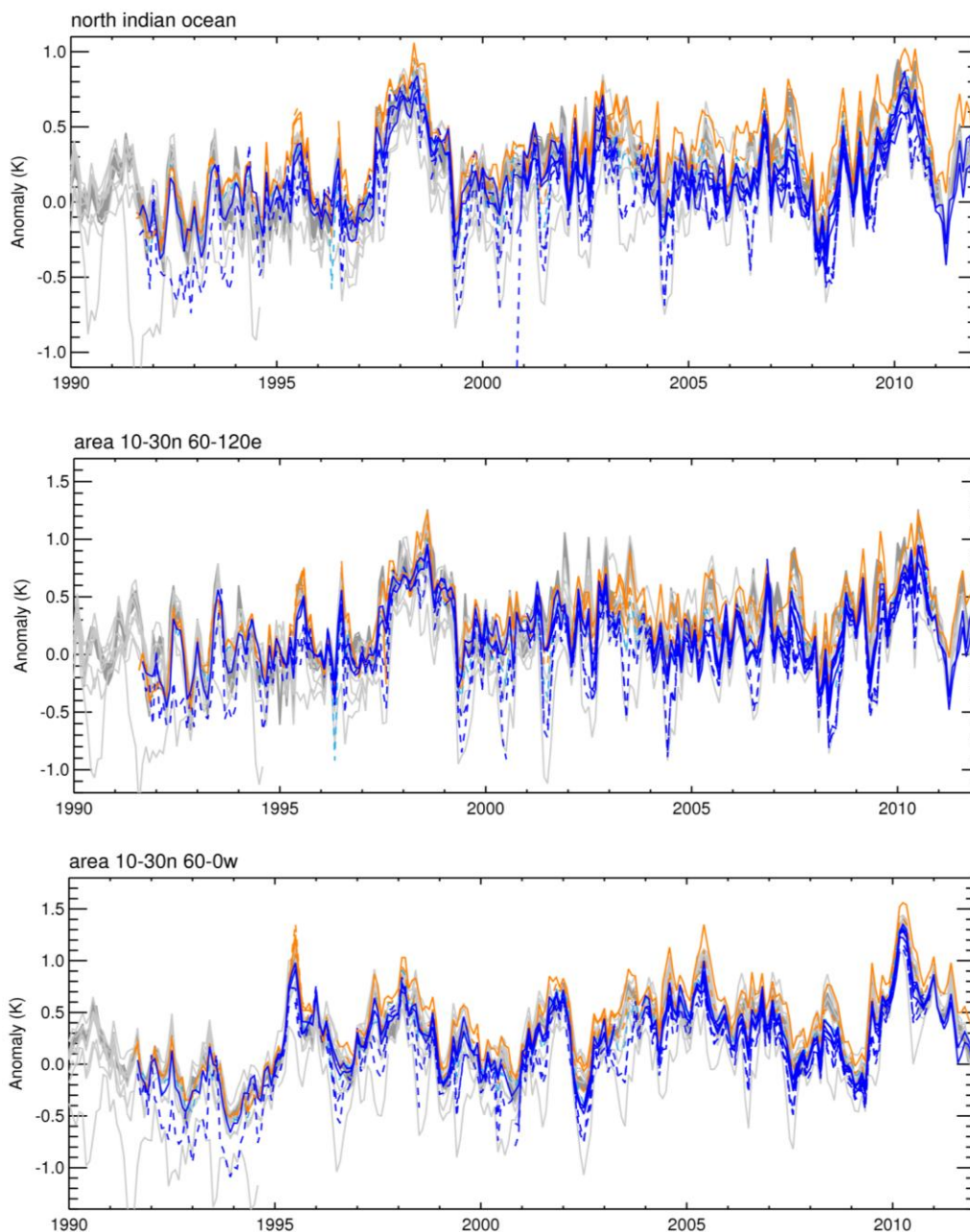
Figure 3-9. Area-average SST anomalies (K) for (top) the North Indian Ocean and regions (middle) 32 and (bottom) 31 described in Figure 3-1, for each of the comparison data sets (grey) and the SST CCI Experimental Release EXP1.2 products [SST CCI ATSR (L3U): orange, SST CCI AVHRR (L2P): blue]. Precursor products from the Phase 1 SST CCI Release LT version 1.0 are shown as dashed lines (these include the Phase 1 SST CCI analysis (L4): green).

3.4.2   MULTI-YEAR AVERAGES

The multi-year averages calculated for this analysis (of which a subset are presented in this section) provide a useful means for assessing spatially the relative biases and multi-year variability in the different data sets considered. In particular, five-year averages expressed as differences relative to the 1991-1995 average for each dataset help to isolate the signal of multi-year variability (
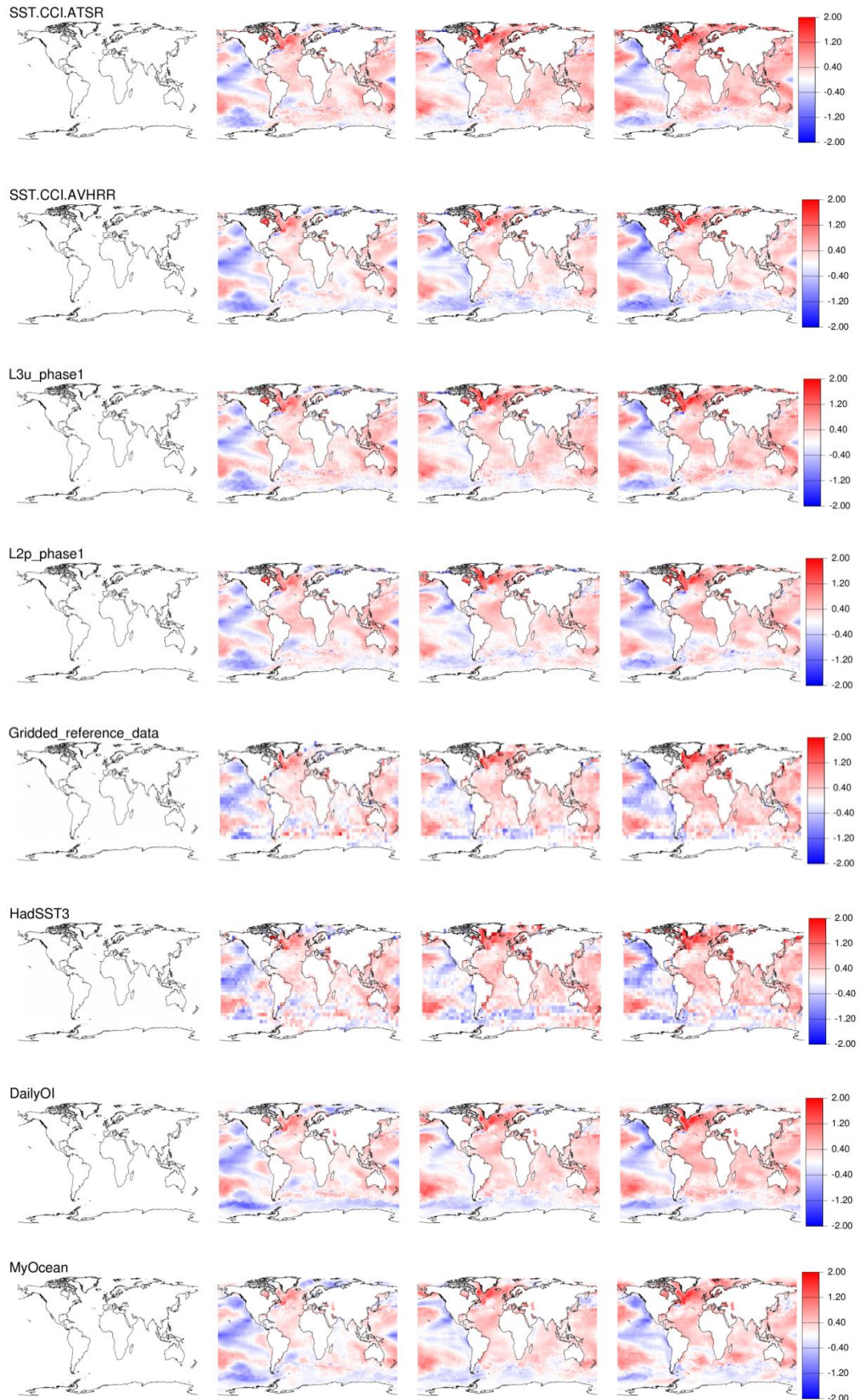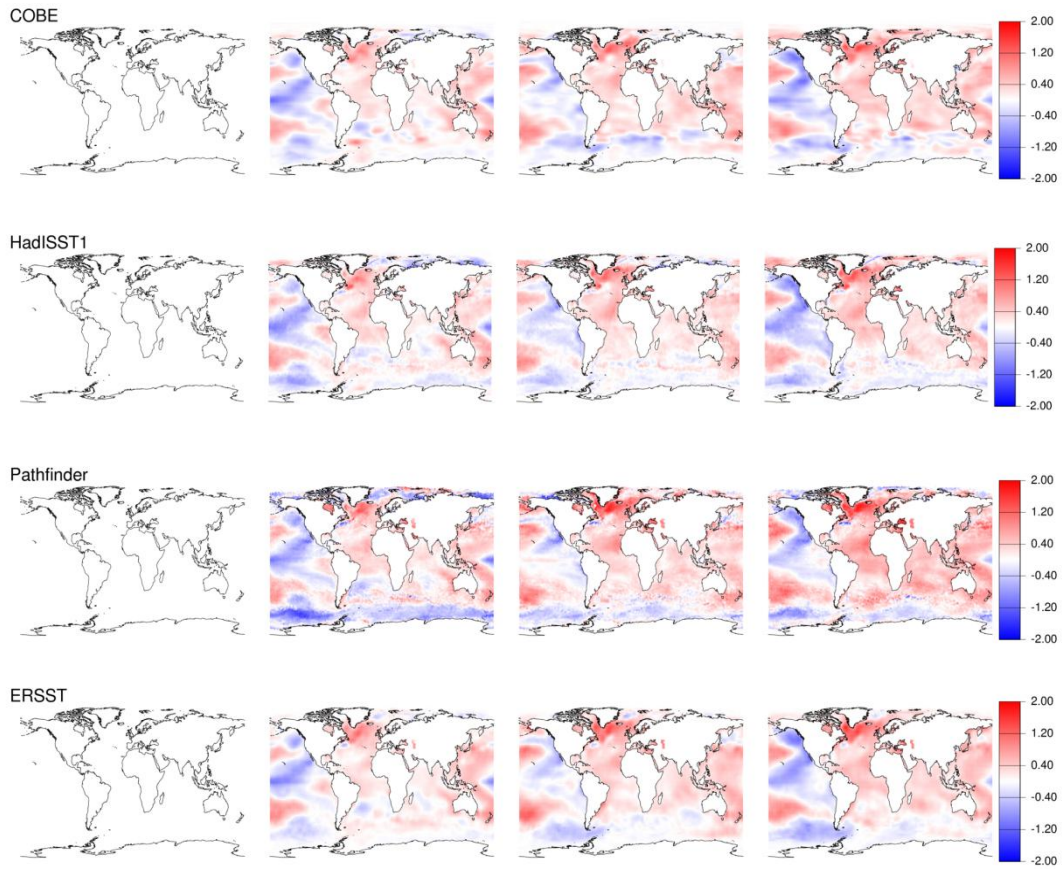
Figure 3-10), decadal averages expressed relative to a common climatology explore both the decadal variability and relative biases between datasets (
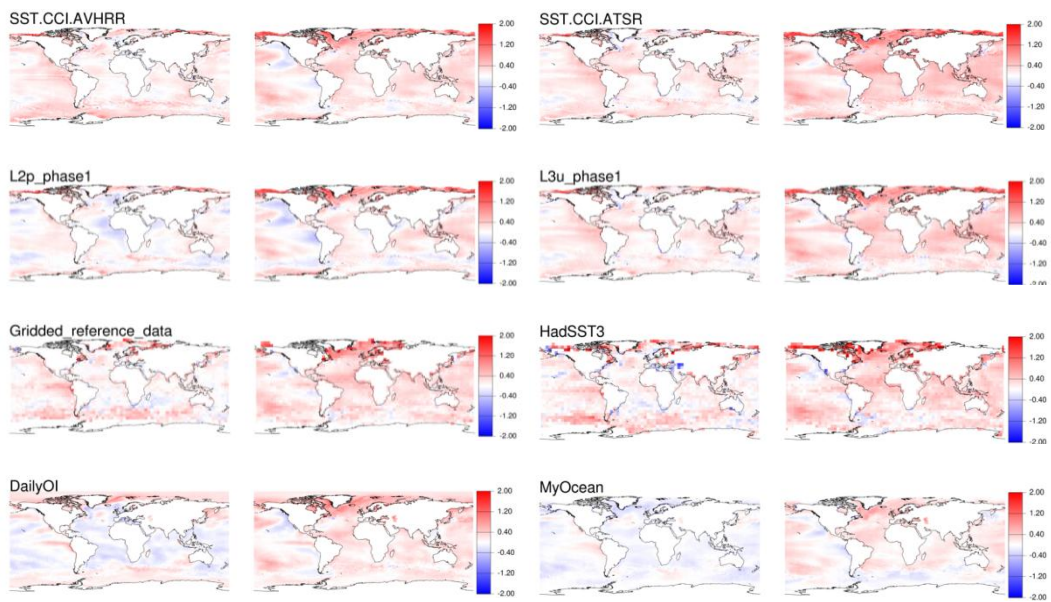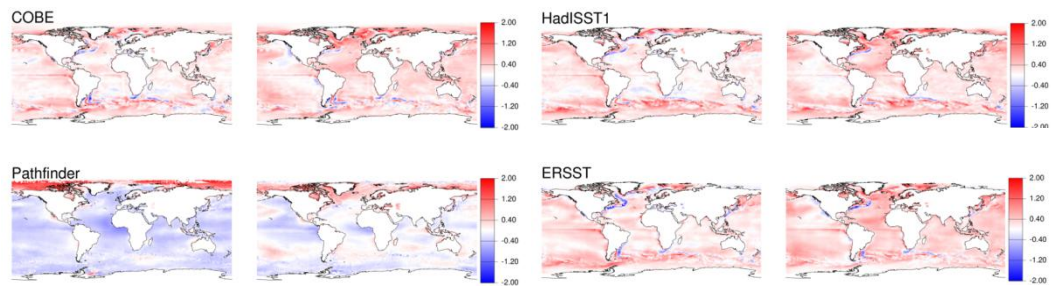
Figure 3-11), and decadal average differences between datasets isolates their relative biases (Figure 3-12). As expected from the time series results (Section 3.4.1) and assessments made in the Phase 1 CAR [RD.371], the Pathfinder, MyOcean OSTIA reanalysis and Daily OI comparison data sets are generally cooler than other datasets, In terms of climate variability over the 1991-2010 period of interest, several known patterns will affect the multi-year average SST anomaly maps (
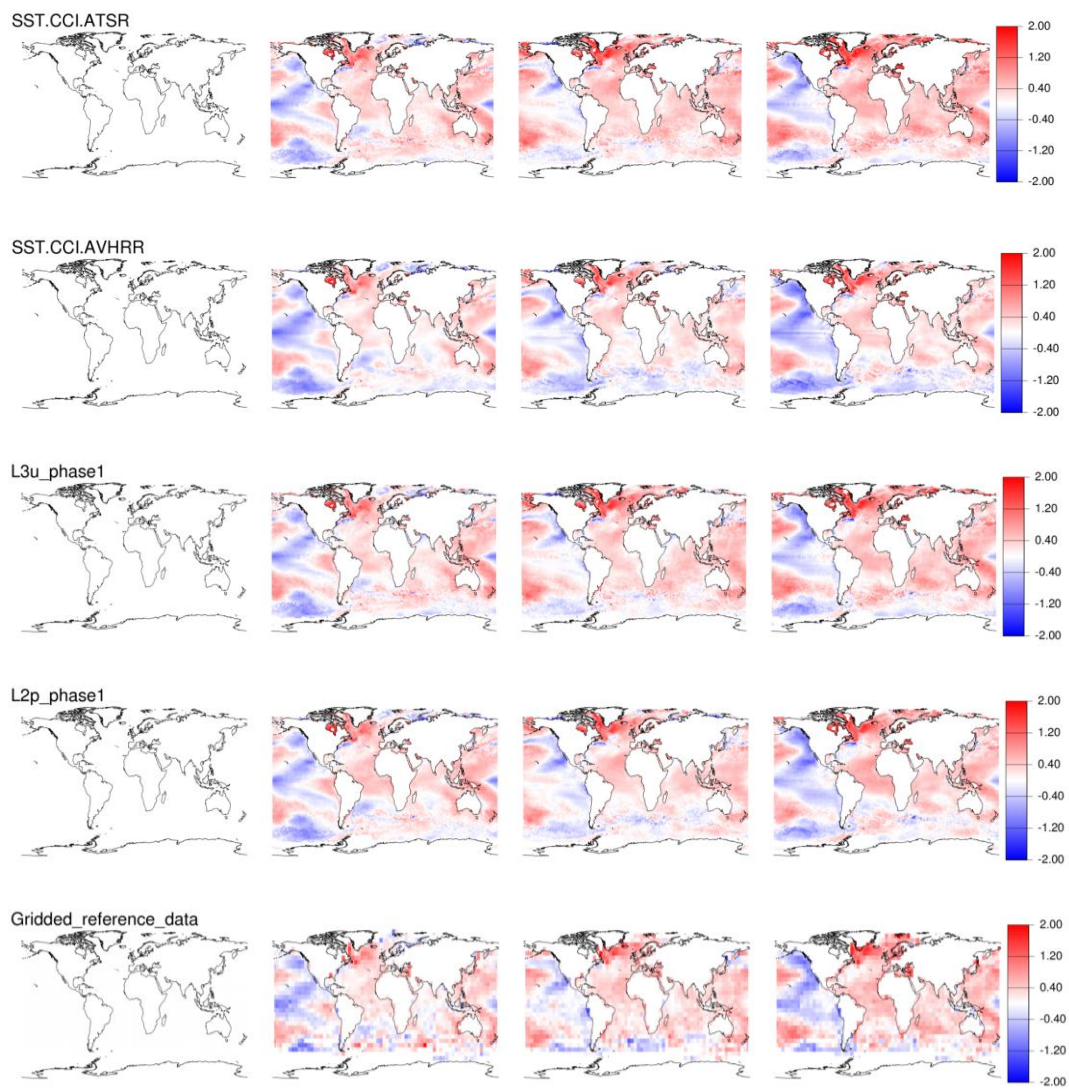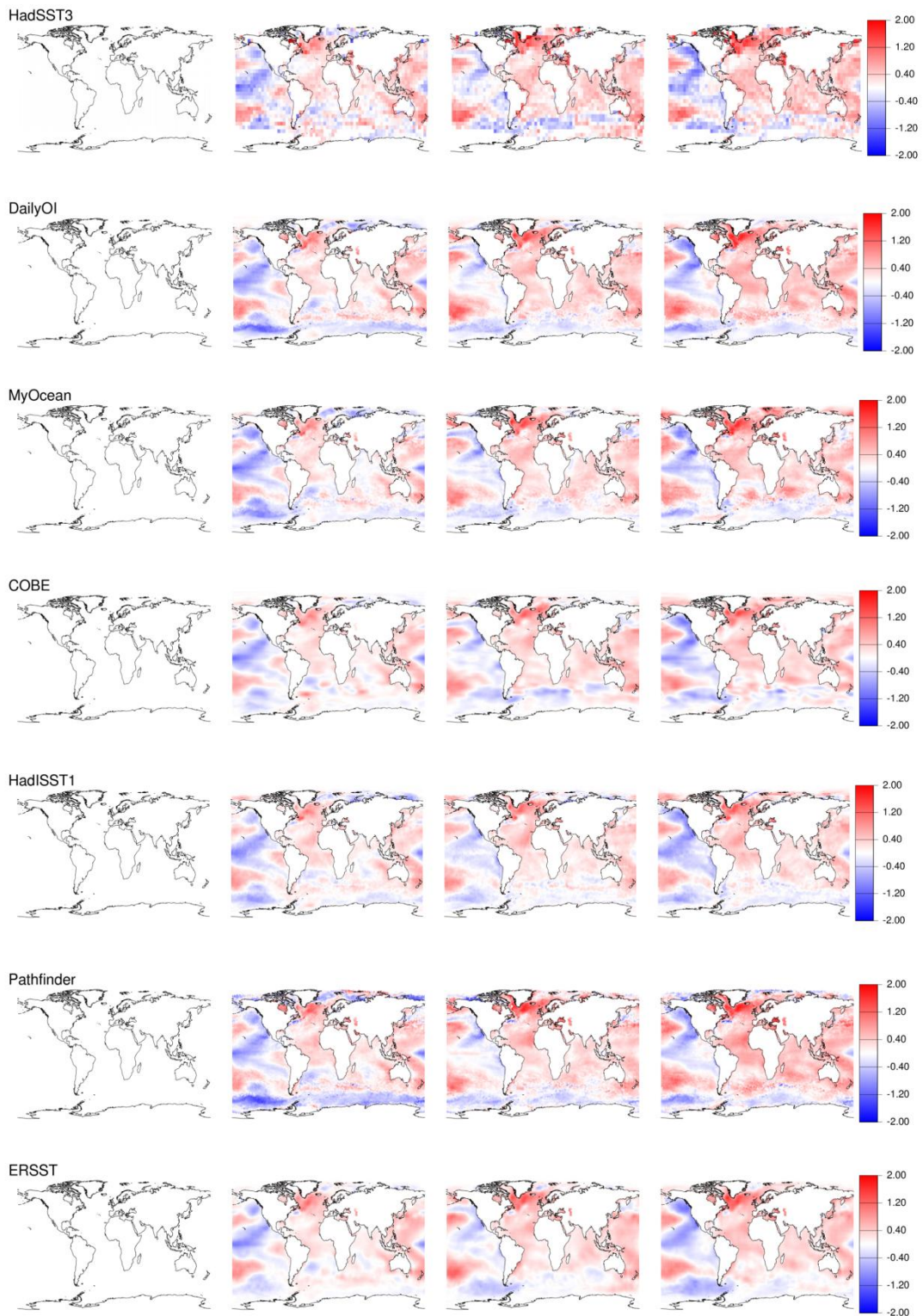
Figure 3-10), including:

- A switch from positive to negative phase of the Pacific Decadal Oscillation during the mid-late 1990s. During positive/negative phase SSTs are anomalously cool/warm in the interior North Pacific (with a weaker signal in the interior South Pacific) and

anomalously warm/cool along the North American Pacific Coast and in the central tropical Pacific.

- A switch from negative to positive phase of the Atlantic Multidecadal Oscillation through the 1990s-2000s. During positive/negative phase SSTs are anomalously warm/cool in the North Atlantic Ocean, in particular in the region of the subpolar gyre. During this period the North Atlantic Oscillation has also switched from a positive to neutral/negative state (albeit with significant interannual variability). A positive state is associated with a tripole SST pattern in the North Atlantic, with a cold anomaly in the subpolar region, a warm anomaly in the mid-latitudes centered off Cape Hatteras, and a cold subtropical anomaly between the equator and 30°N.

- Although a dominant source of interannual variability, fingerprints of the ENSO phenomena are also expected in multi-year SST anomalies. During an El Niño/La Niña event SSTs are anomalously warm/cool over the central and eastern tropical Pacific. A strong El Niño event occurred in 1997/1998 followed by successive La Niñas from 1998-2000, and a sequence of La Niña–El Niño–La Niña events occurred over the period 2007-2011. El Niño events also occurred in 1991-1992 and 2002-2003.

- SST anomalies observed in the South Pacific sector around 40°-70°S and 90°-170°W have been related to ENSO teleconnections and the Southern Annular Mode, though the relationships with each phenomena may change with time [Yeo and Kim, 2015; RD.389].

- Summer Arctic Sea Ice extent has shown a general reduction over the 1991-2010 period, with a pronounced minimum in 2007. Warming of the exposed ocean will lead to warm SST anomalies.

The multi-year variability, shown in
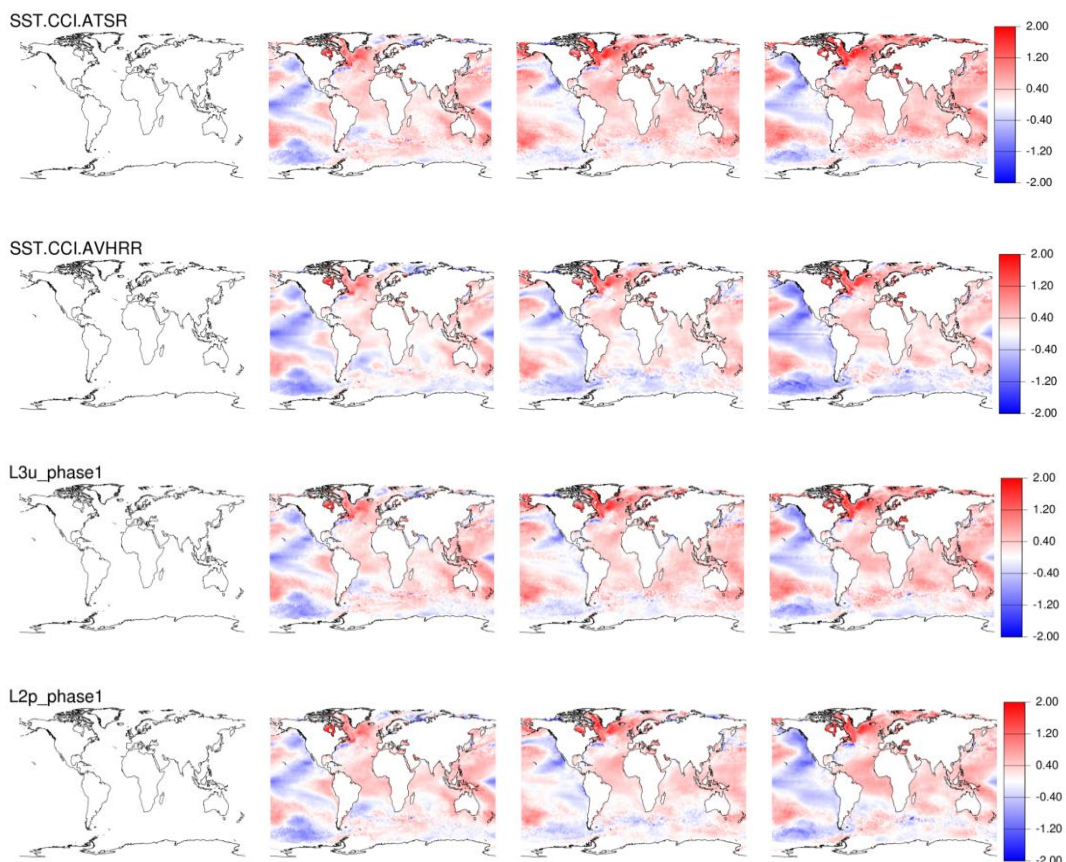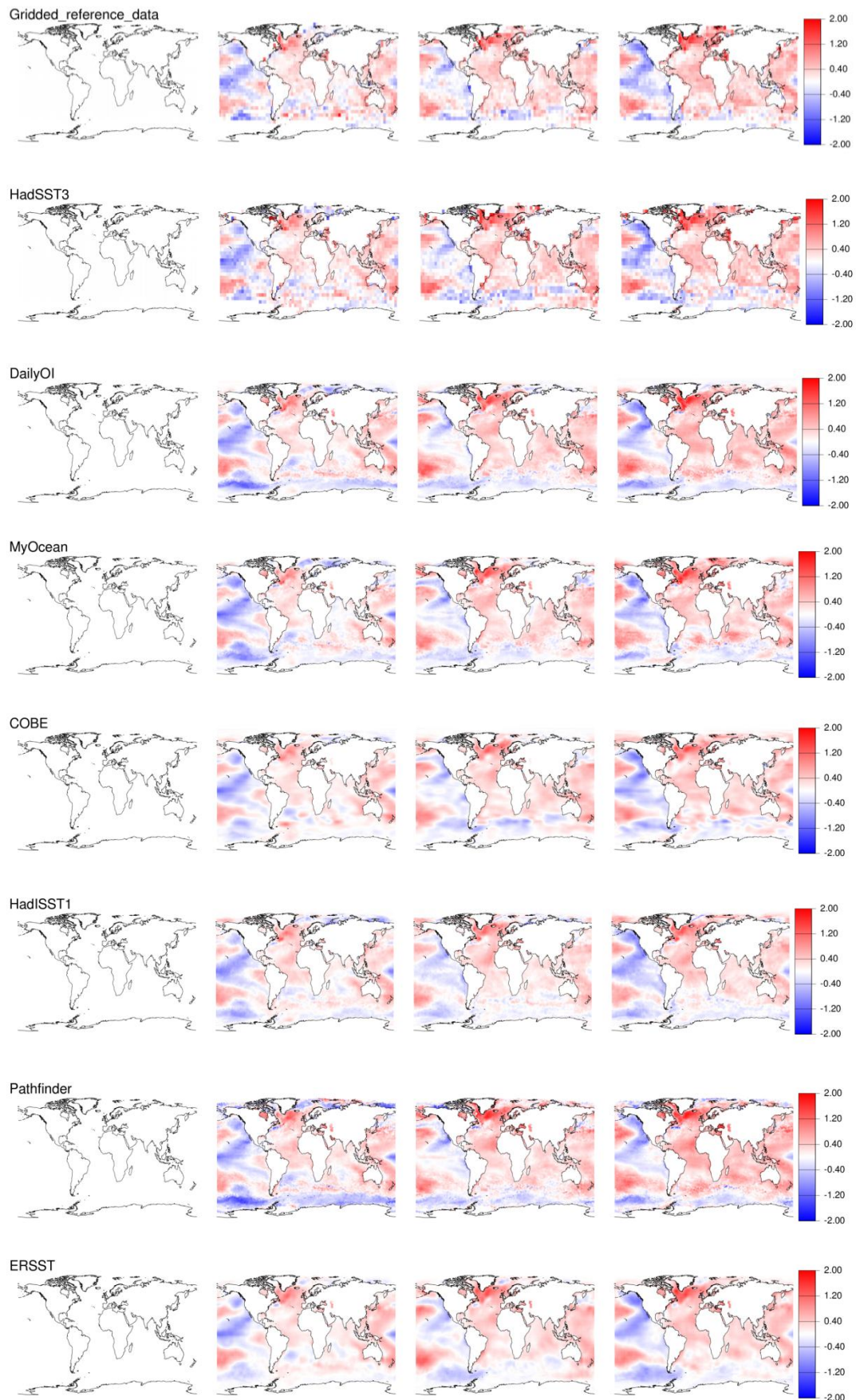
Figure 3-10, is typically larger than the relative biases seen in the large-scale averages and is generally consistent between the SST CCI products and the comparison data sets. From the 1991-1995 baseline, the later periods are generally characterised by cooling in the central and north-eastern Pacific, cooling in the South Pacific sector of the Southern Ocean, and warming in most other areas. There is some evidence of cooling elsewhere in the Southern Ocean but the exact details of this appear variable between datasets. Changes in the Pacific Ocean partly reflect a switch to the negative phase of the Pacific Decadal Oscillation. The North Atlantic is especially warm, warming faster (Figure 3-3) than the other ocean basins since 1991, reflecting the switch to the warm phase of the Atlantic Multidecadal Oscillation [Knight et al., 2005; RD.356].

If the spatial patterns of multi-year variability for the SST CCI ATSR and SST CCI AVHRR data sets are inter-compared for different 5-year periods (
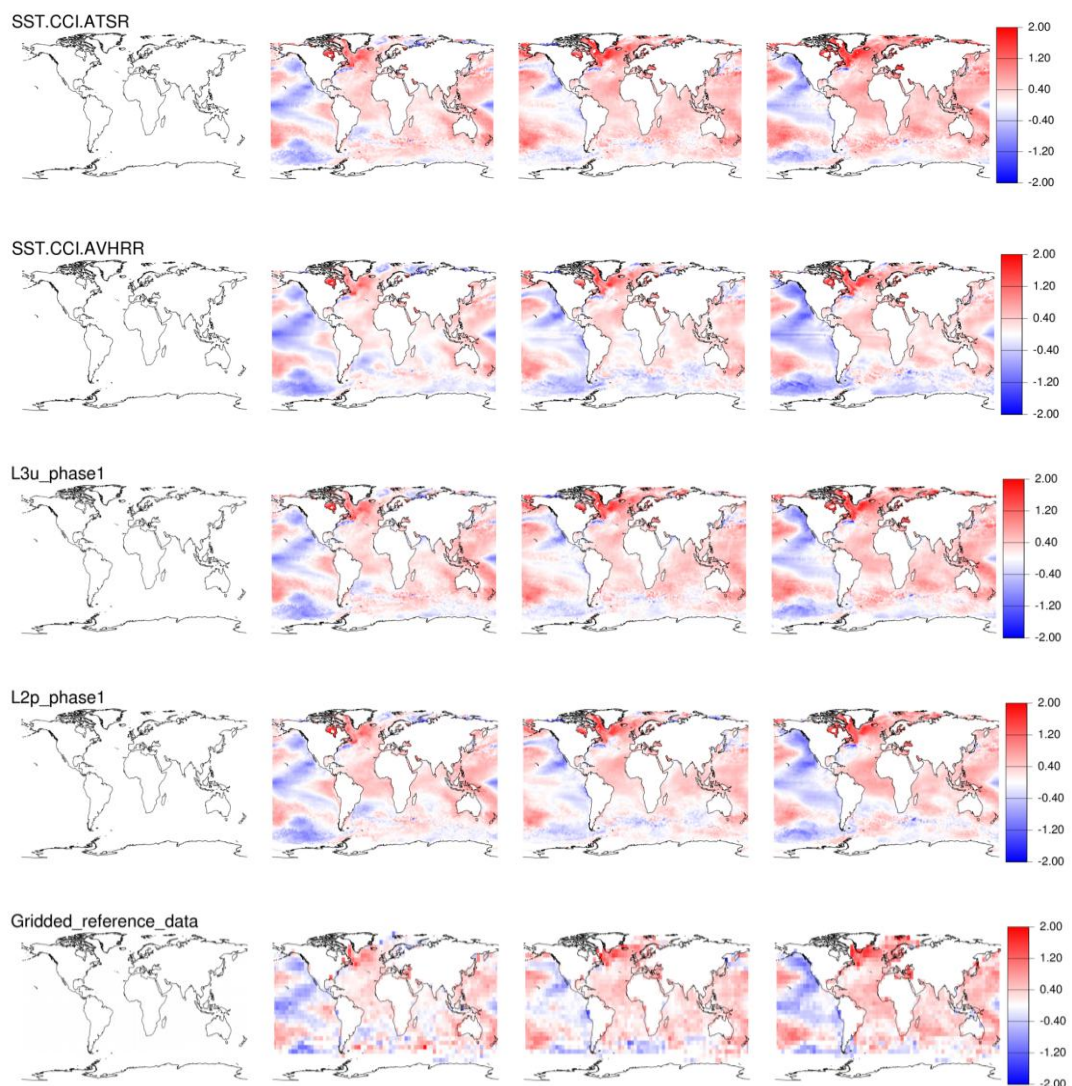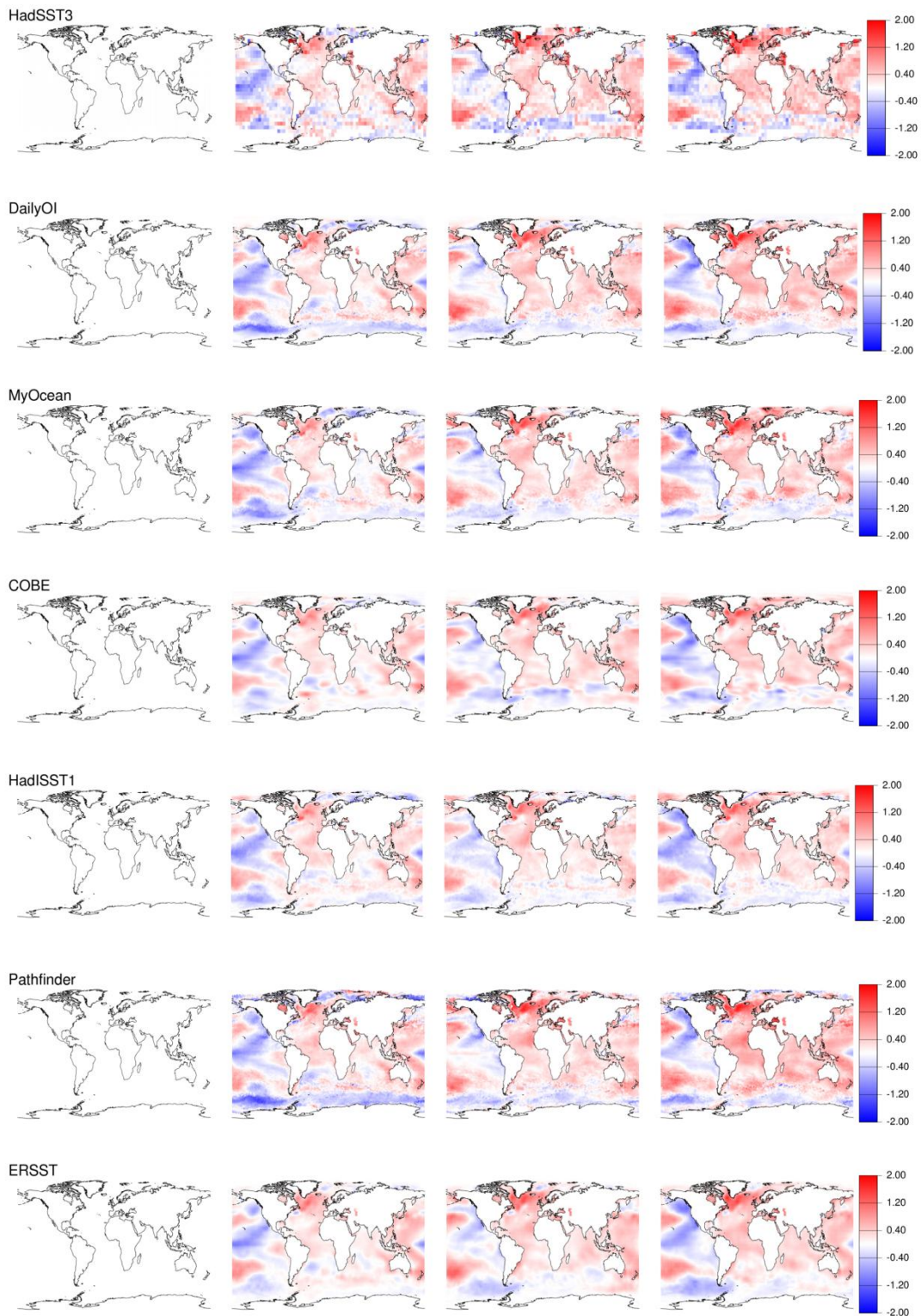
Figure 3-10), generally regions where the AVHRR is cool appear cooler and regions where the ATSR is warm appear warmer. These differences are most pronounced in more recent 5-year periods and seem attributable to the diverging trends seen in the two datasets in all ocean basins (Figure 3-3). The multi-year variability seen in the SST CCI

ATSR and SST CCI AVHRR products is also comparable to their Phase 1 precursors, though some differences are evident for the AVHRR product (described below).

Looking more closely at individual 5-year periods (
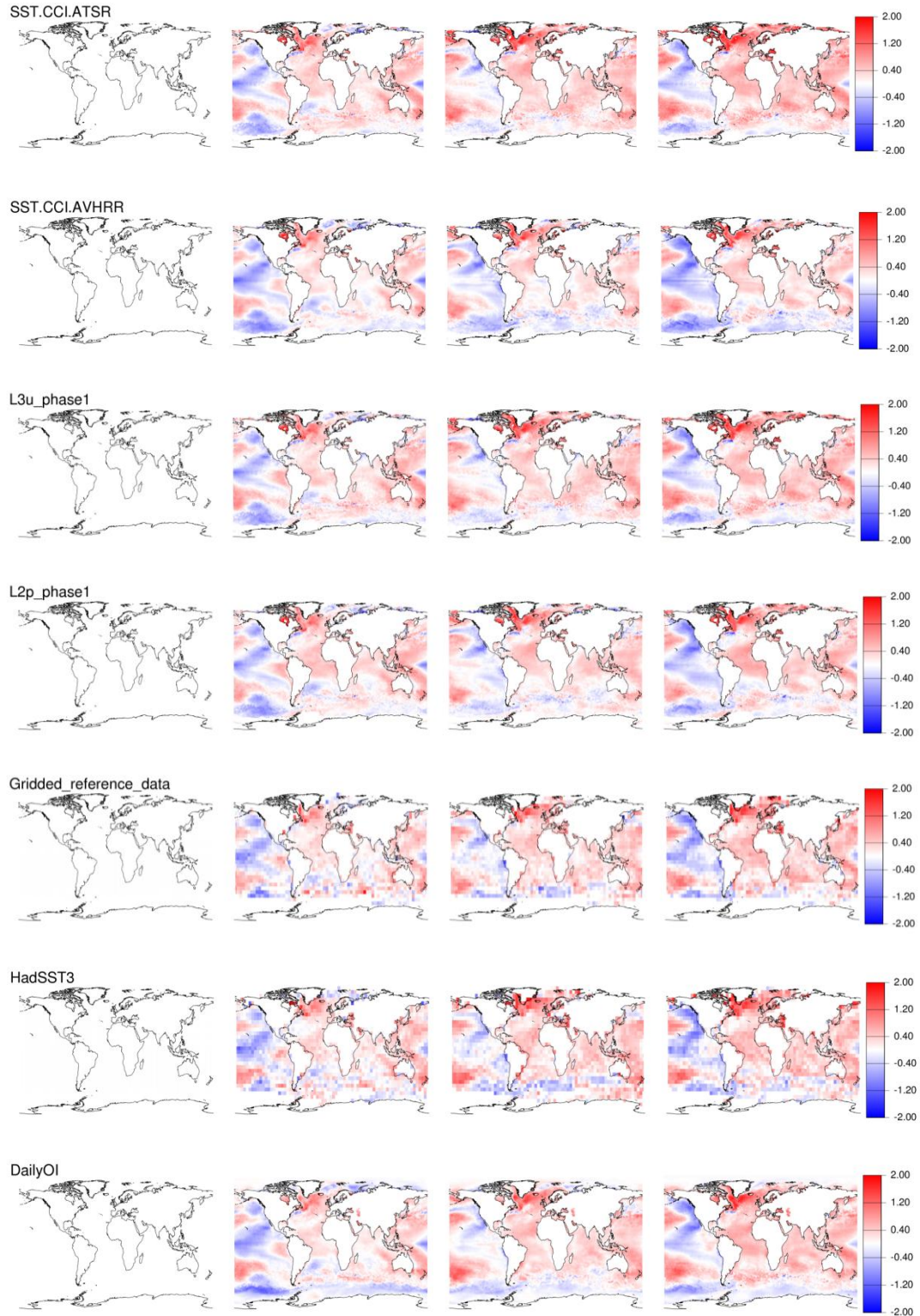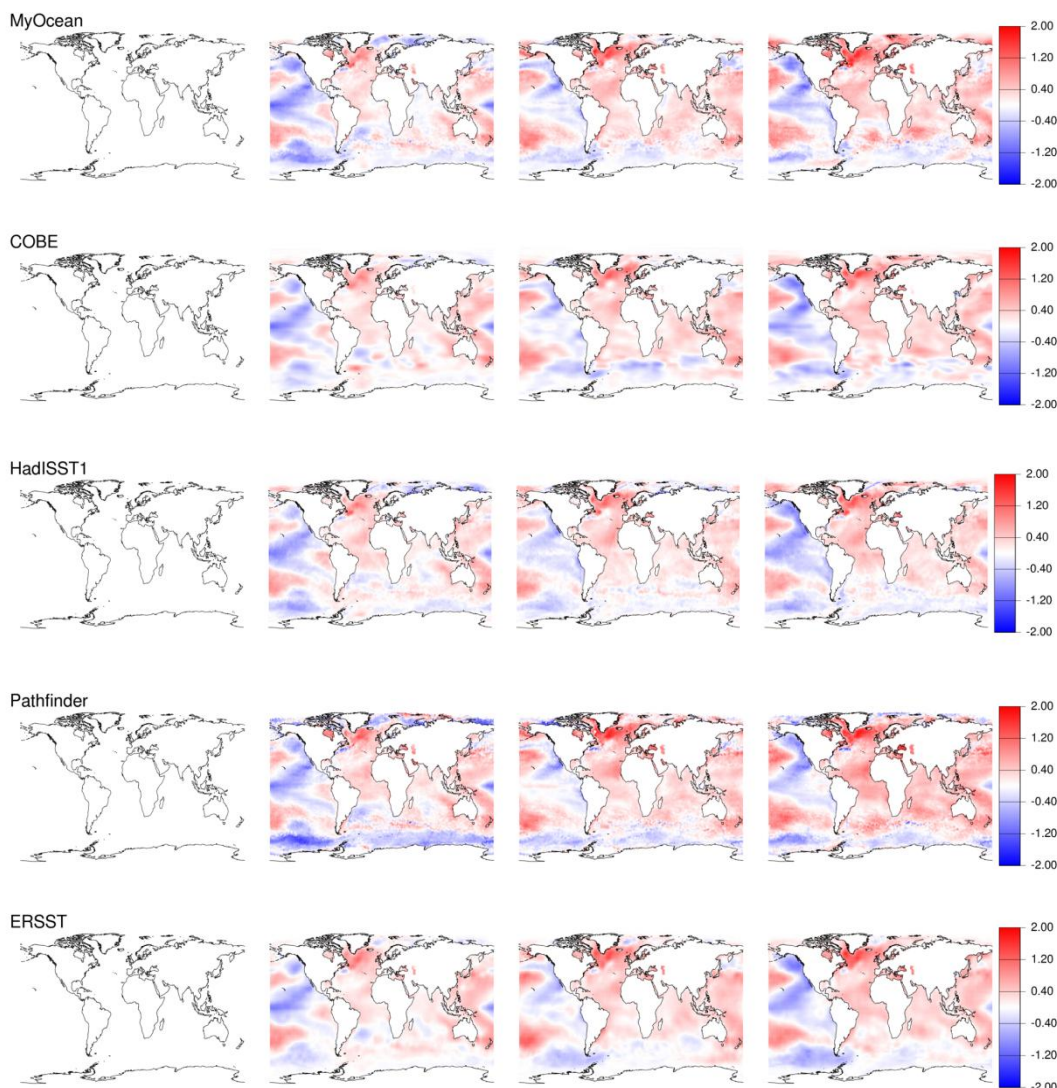
Figure 3-10):

- In the 1996-2000 period, there is a strong cool band in the southern Ocean eastern hemisphere which is present in the Pathfinder and Daily OI data sets (the latter includes Pathfinder), but less pronounced, or absent in others.
- In the 2001-2005 period, the SST CCI AVHRR product is cooler in the eastern tropical Pacific relative to its Phase 1 precursor. This gives a better agreement with the comparison datasets, which generally show a cool anomaly east of the dateline in the central Pacific with the exception of Pathfinder and SST CCI ATSR. For the SST CCI ATSR product this seems partly due to the warming trend discussed above, which acts to diminish the signature of cool features.
- In the 2006-2010 period, the SST CCI AVHRR product is cooler in the eastern hemisphere of the Southern Ocean relative to its Phase 1 precursor, however the comparison datasets show a range of variability at this location so it is difficult to say if the latest reprocessing is an improvement. Some interesting differences are also seen in the eastern tropical Pacific. In the SST CCI AVHRR, MyOcean and HadISST datasets a cool anomaly is seen in this location, whilst in the HadSST3, Pathfinder and Daily OI datasets a faint warm anomaly is observed. For the other datasets relatively little anomaly is seen. It is not clear what explains this range of results.
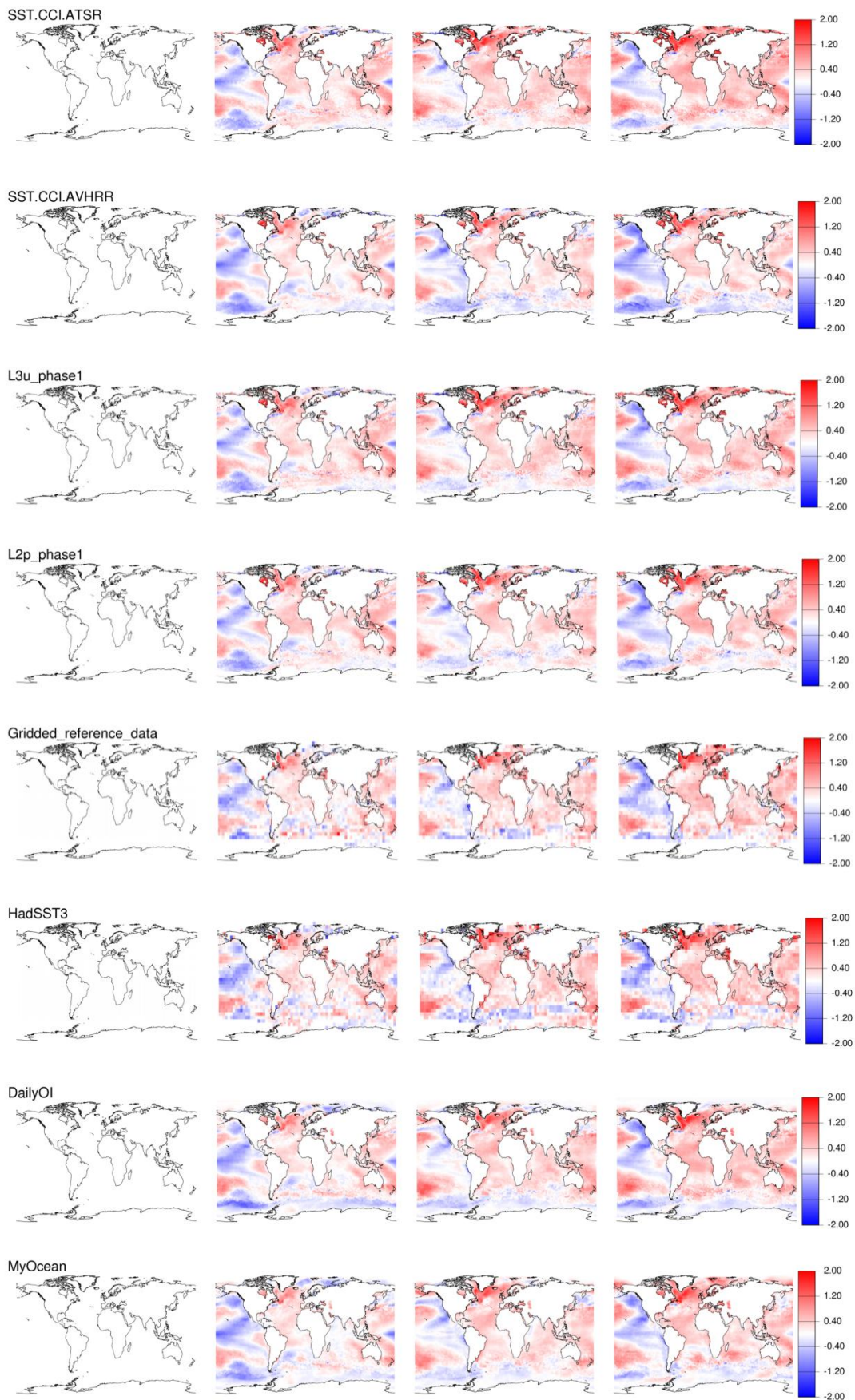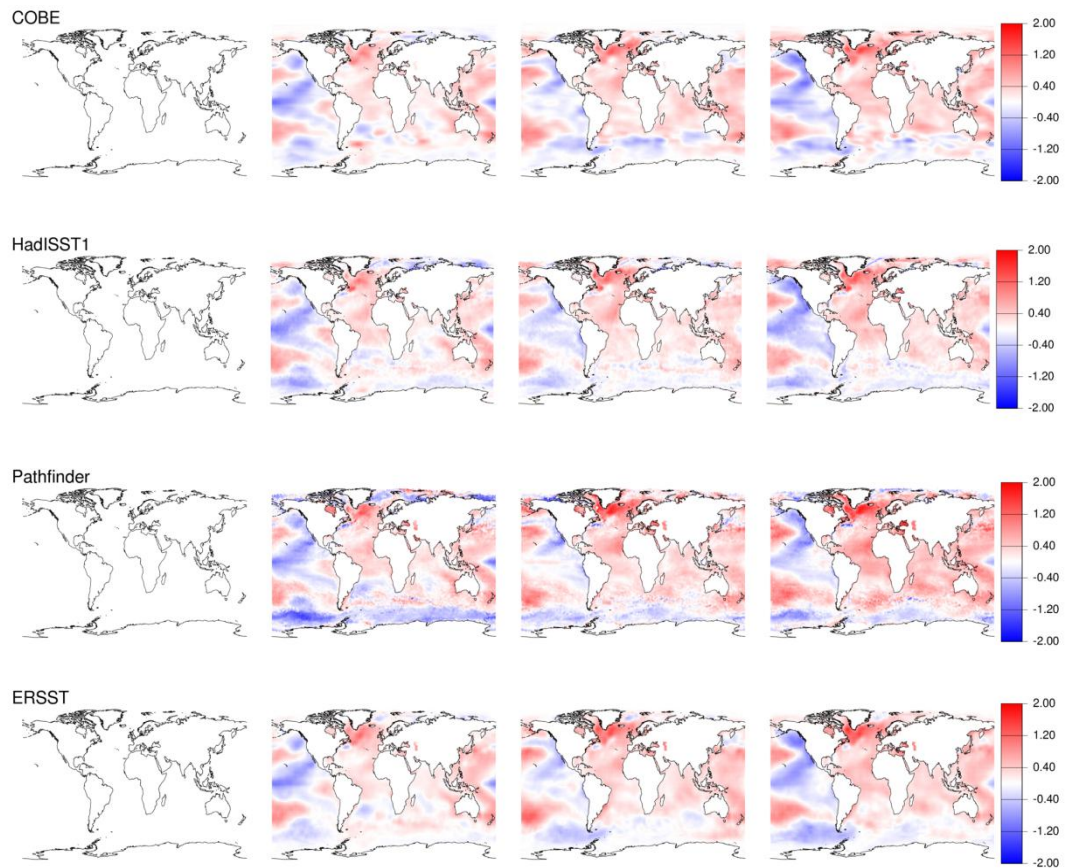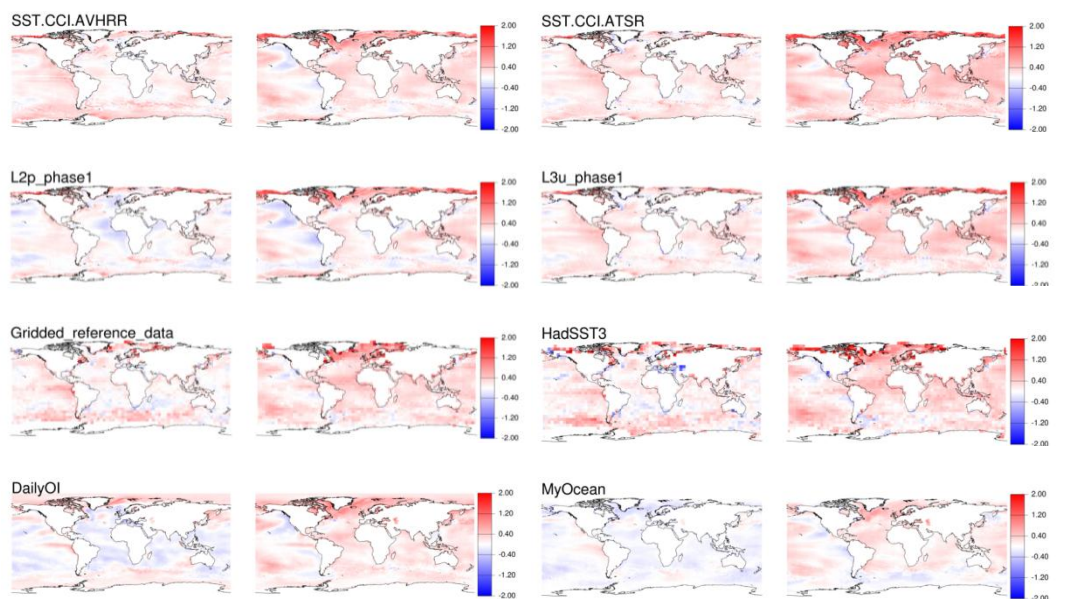
Figure 3-10. 5-year average SST anomalies (K) relative to the average for 1991-1995 for a selection of data sets, including precursor products from the Phase 1 SST CCI Release LT version 1.0. From left to right the periods are: 1991-1995, 1996-2000, 2001-2005, and 2006-1010. For a pixel to be filled, more than 30% of months need to have a valid SST.
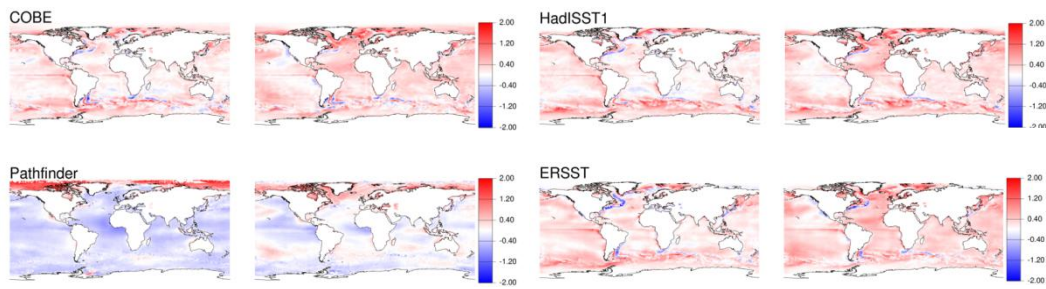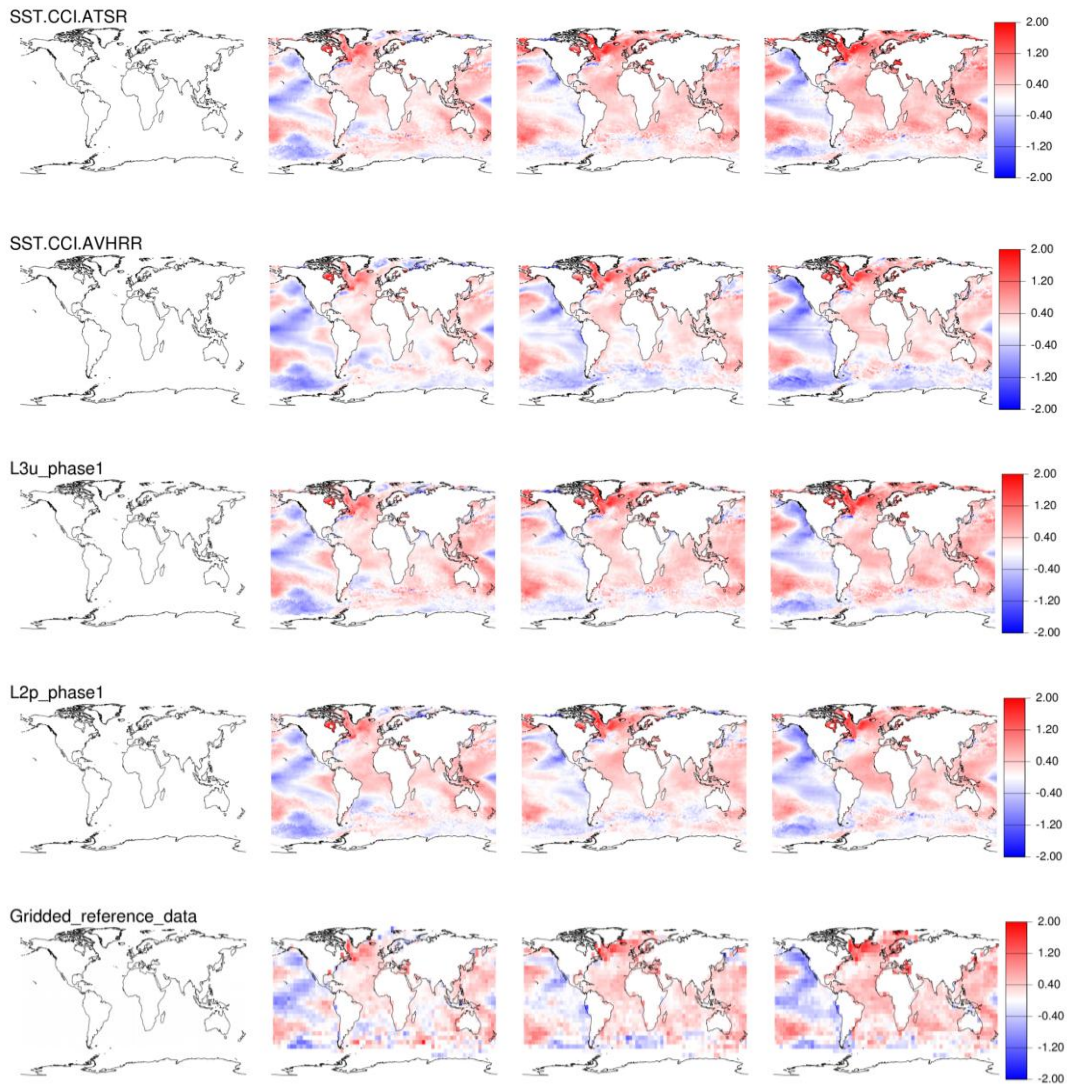
Decadal averages are shown in

Figure 3-11 as anomalies relative to the MyOcean OSTIA reanalysis climatology. This mainly highlights the relative biases and trends amongst the data sets. The relative coolness of the Pathfinder dataset is particularly obvious, and the relative warmness of the SST CCI ATSR dataset (and ERSST) in the later 2001-2010 period is also apparent. The decadal variability appears reasonably consistent amongst the different datasets, with the changing phase of the Pacific Decadal Oscillation the most apparent feature. This is consistent with the good agreement seen amongst datasets for multi-year variability discussed above (
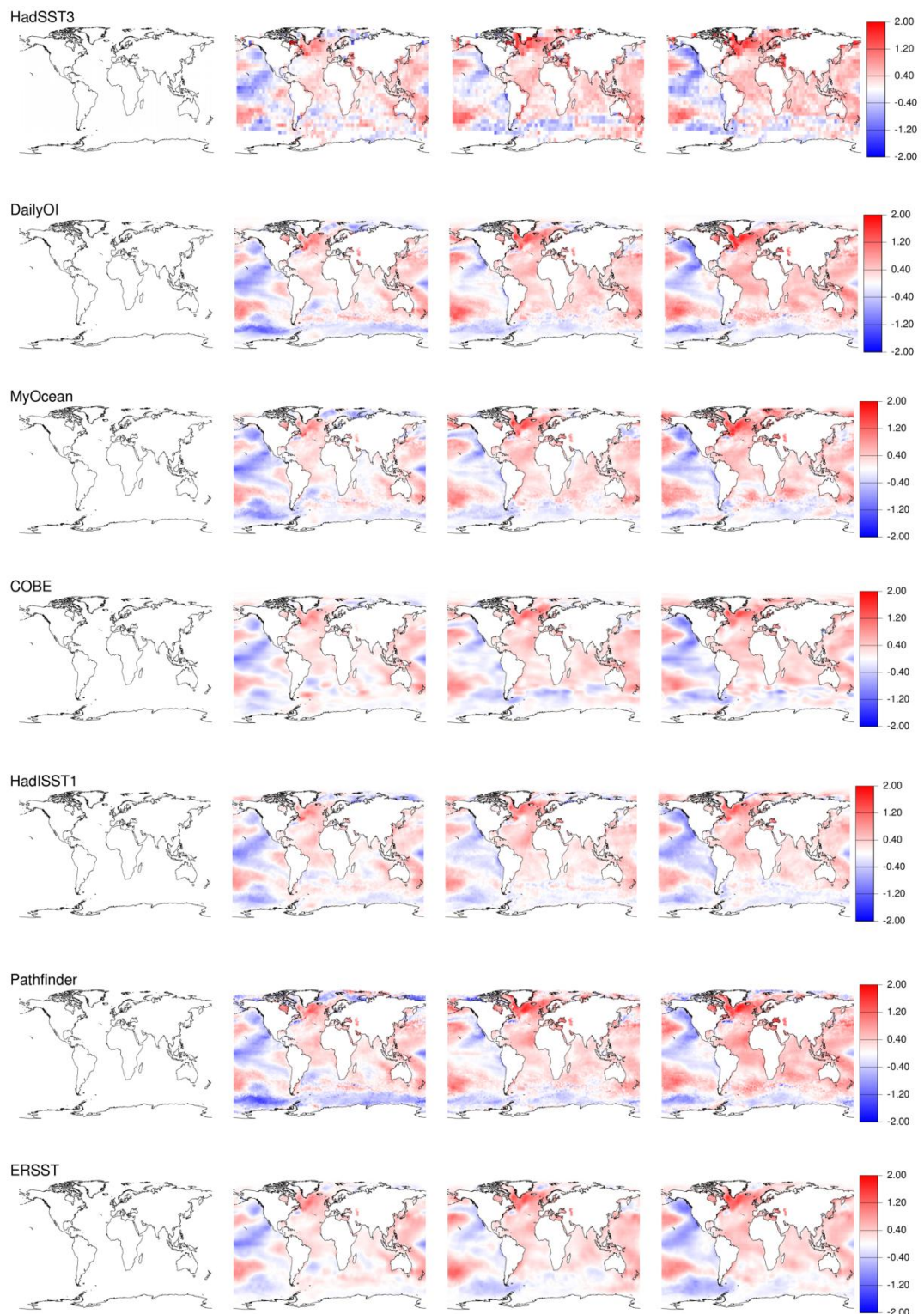
Figure 3-10).

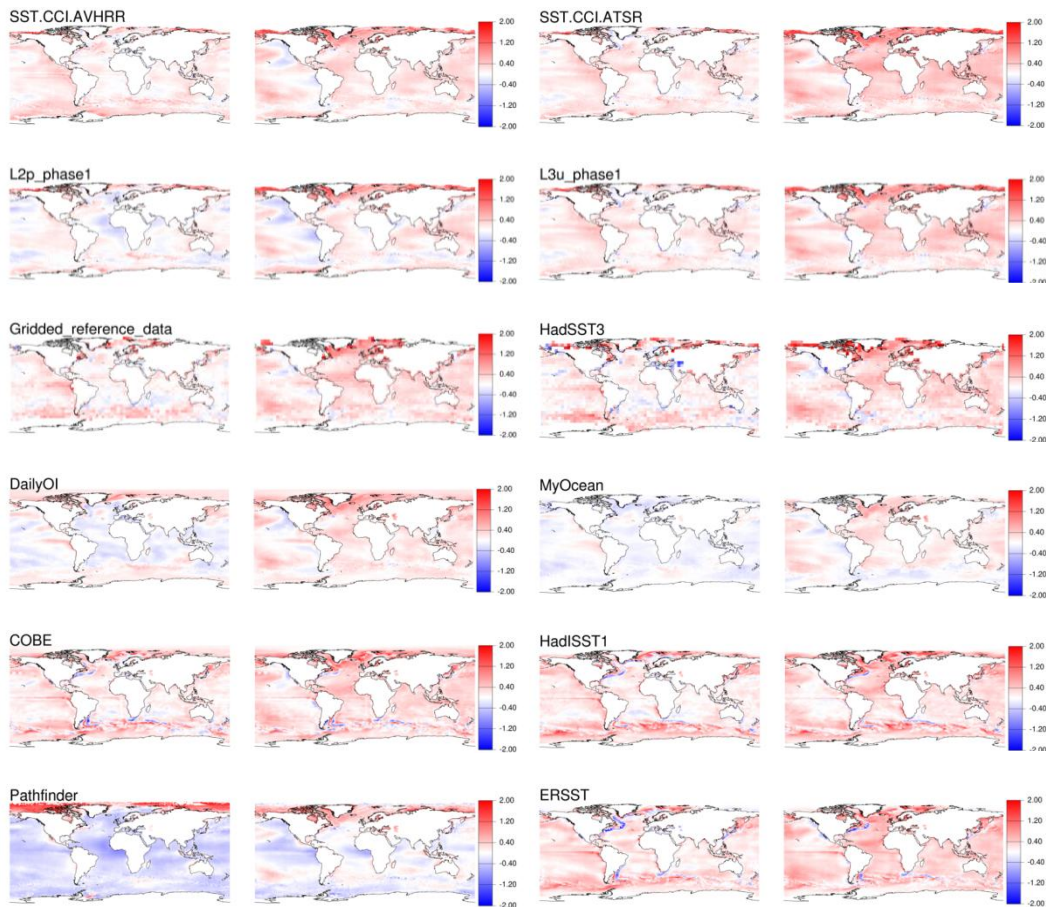Relative to their Phase 1 precursors, the SST CCI ATSR decadal averages shown in

Figure 3-11 are reasonably comparable. The 2001-2010 decadal average for SST CCI AVHRR is also relatively comparable to its Phase 1 precursor, albeit generally warmer, consistent with the generally warmer global average anomalies seen in Figure 3-2 for the latest AVHRR product. For the 1991-2000 decadal average, the SST CCI AVHRR product shows larger differences relative to its Phase 1 precursor than for the 2001-2010 decadal average. In particular, cool anomalies in the North Pacific, eastern tropical Atlantic and parts of the Indian Ocean in the Phase 1 product are no longer evident in the latest reprocessing and the Southern Ocean is also generally warmer in the latest product. This difference is consistent with the removal of a large cool global bias prior to 1995 in the latest SST CCI AVHRR product which was described in Section 3.4.1.
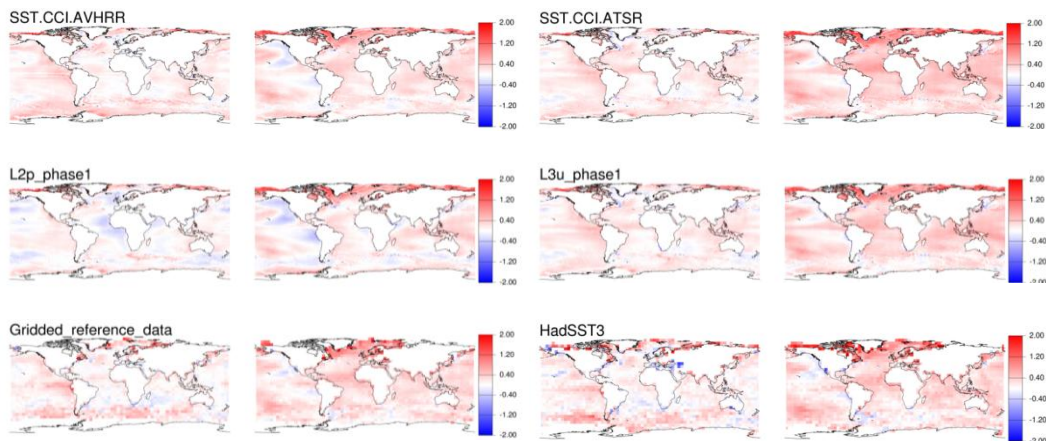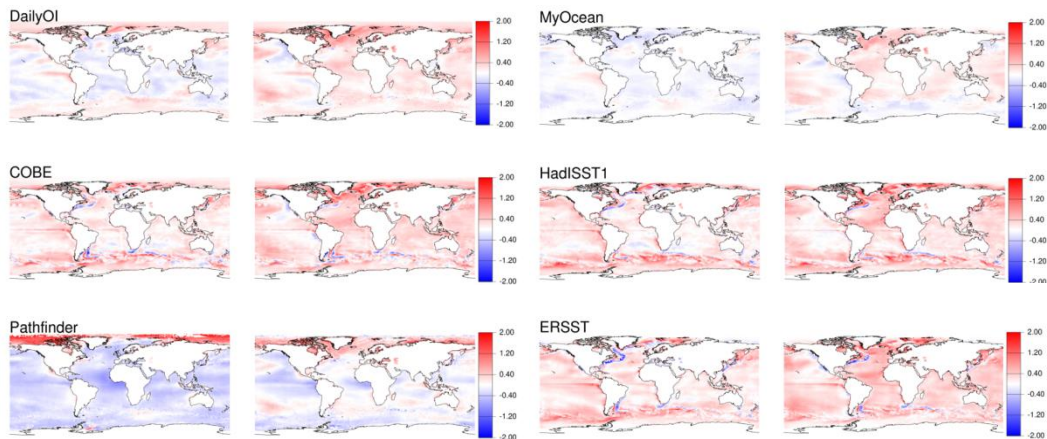
Figure 3-11. Decadal average SST anomalies (K) for a selection of data sets including precursor products from the Phase 1 SST CCI Release LT version 1.0. From left to right the periods are 1991-2000, 2001-2010 (note that each row contains two data sets). For a pixel to be filled, more than 30% of months need to have a valid SST.

The thumbnail collocated decadal average differences shown in Figure 3-12 and Figure 3-13 provide a convenient way to compare different products for the 1991-2000 and 2001-2010 periods and to discern any features particular to some dataset. For example, the known cool bias of Pathfinder relative to other datasets is clearly apparent.

For 1991-2000 (Figure 3-12), both the SST CCI ATSR and SST CCI AVHRR products show some evidence of warmth in the lower latitudes, and particularly coolness in the higher latitudes, relative to most of the comparison data including the gridded in situ datasets (but excluding MyOcean and DailyOI which are generally cool). It is difficult to attribute the high latitude coolness as a feature of the SST CCI products given limited *in situ* sampling in these latitudes. Nevertheless, the high latitudes are challenging for thermal infrared observations too: atmospheric conditions are often relatively anomalous compared to the variability in mid and lower latitudes, cloud cover is often high, so that TIR sampling is also relatively limited, and cloud detection conditions are often adverse (low sun angles and polar night) so that cloud contamination effects are potentially greater at higher latitudes. These effects may contribute to satellite SST bias in these regions. The SST CCI ATSR product is broadly warmer in the lower latitudes and cooler in the higher latitudes relative to the SST CCI AVHRR product. This discrepancy between the SST CCI products is reduced relative to that seen for the Phase 1 products. This is due to the removal of a cool bias in the AVHRR data prior to 1995, as discussed above and in Section 3.4.1. In particular a large bias between the Phase 1 products in the eastern tropical Atlantic is no longer evident in the latest SST CCI datasets.

For 2001-2010 (Figure 3-13), the SST CCI ATSR product is warmer globally than the SST CCI AVHRR product. A similar result is seen when comparing the two Phase 1 products, with the exception of the highest latitudes where the AVHRR is warmer than ATSR. This high latitude warmth of the AVHRR is no longer evident in the latest SST CCI products. Compared with its Phase 1 precursor the SST CCI ATSR product is warmer, particularly in the extra-tropics. The SST CCI AVHRR product is also warmer than its Phase 1 precursor, with the exception of the highest latitudes where the aforementioned warmth in the Phase 1 product has been removed. As for 1991-2000, the MyOcean and DailyOI products are relatively cool compared to other datasets.
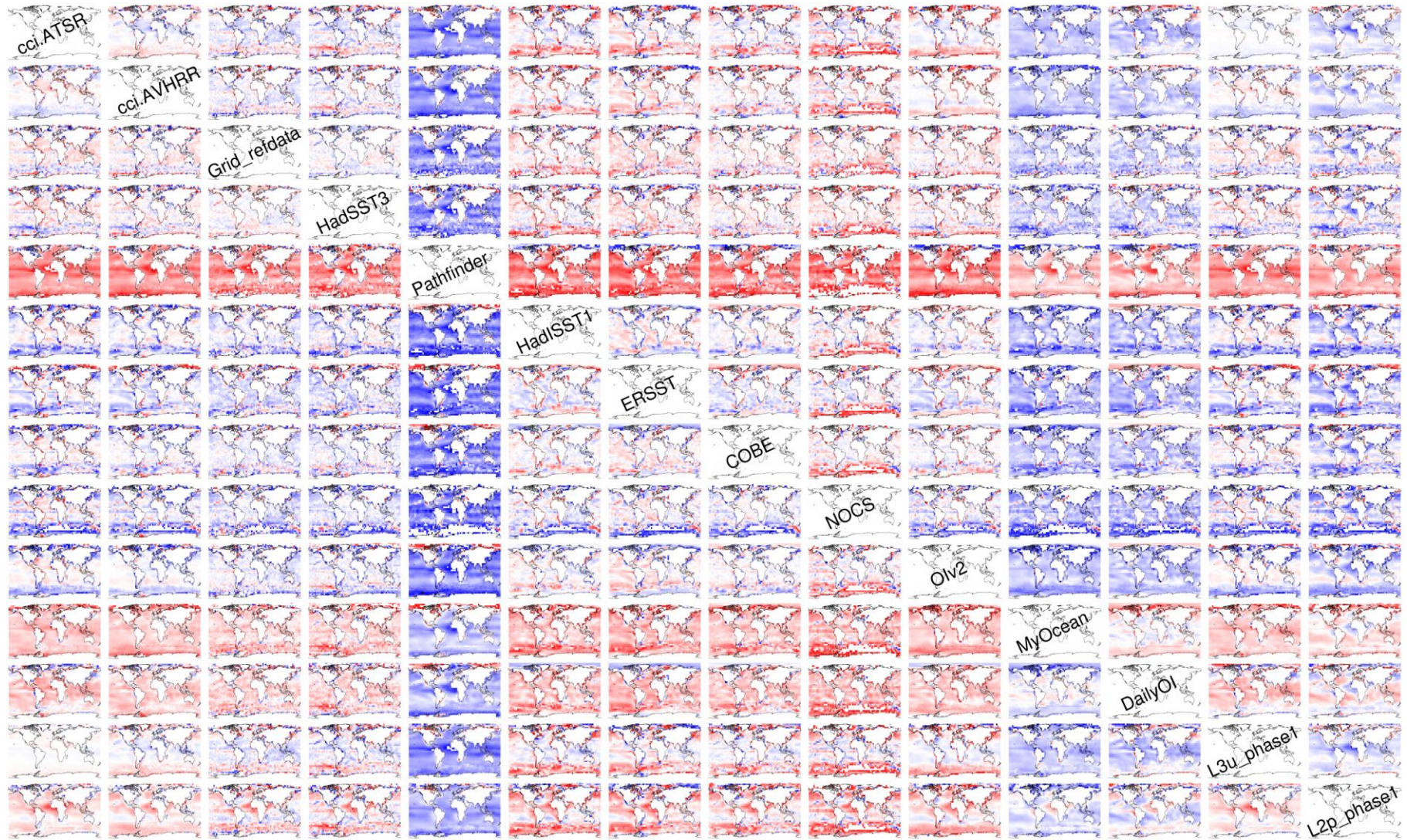
Figure 3-12. Colocated decadal (2001-2010) average differences between all pairs of data sets including precursor products from the Phase 1 SST CCI Release LT version 1.0. Colour scale is -1K to 1K (half the range of
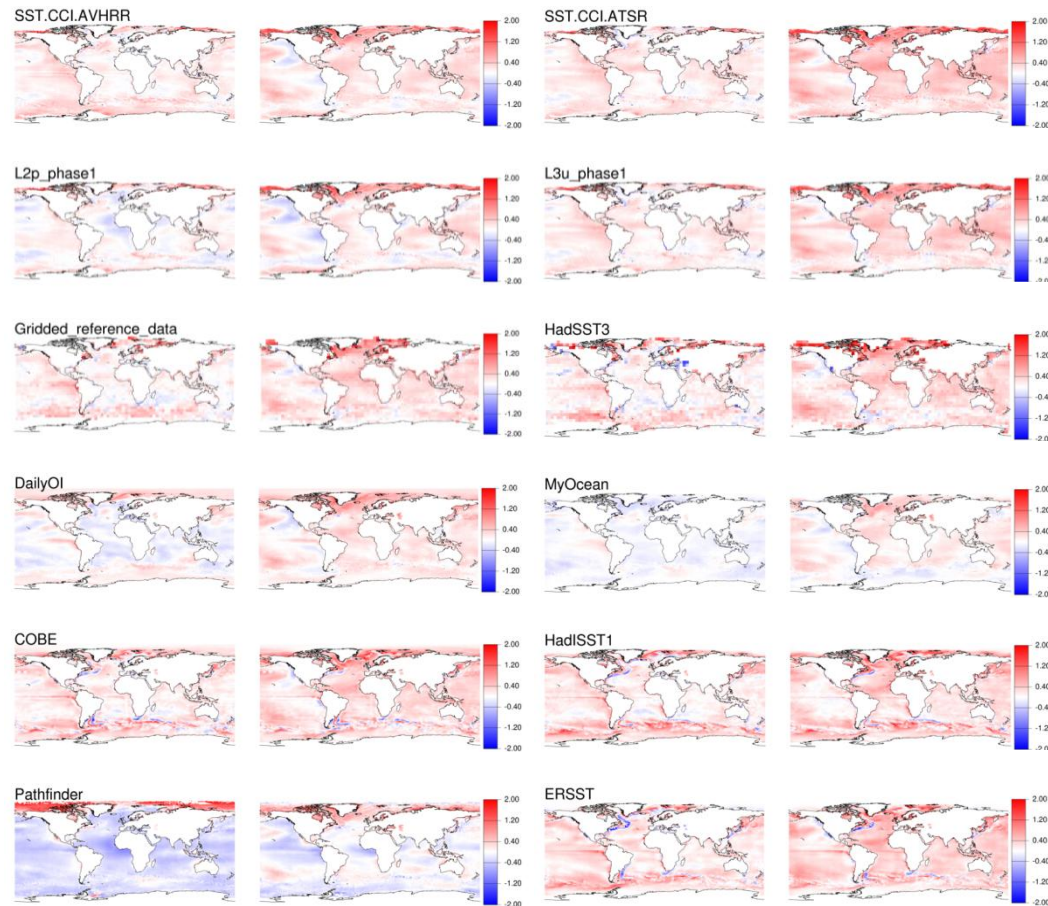

Figure 3-11). The difference is X minus Y, so for example the Pathfinder column is consistently negative because the Pathfinder data set has a cold bias relative to all the other data sets (i.e. Pathfinder minus other data set)
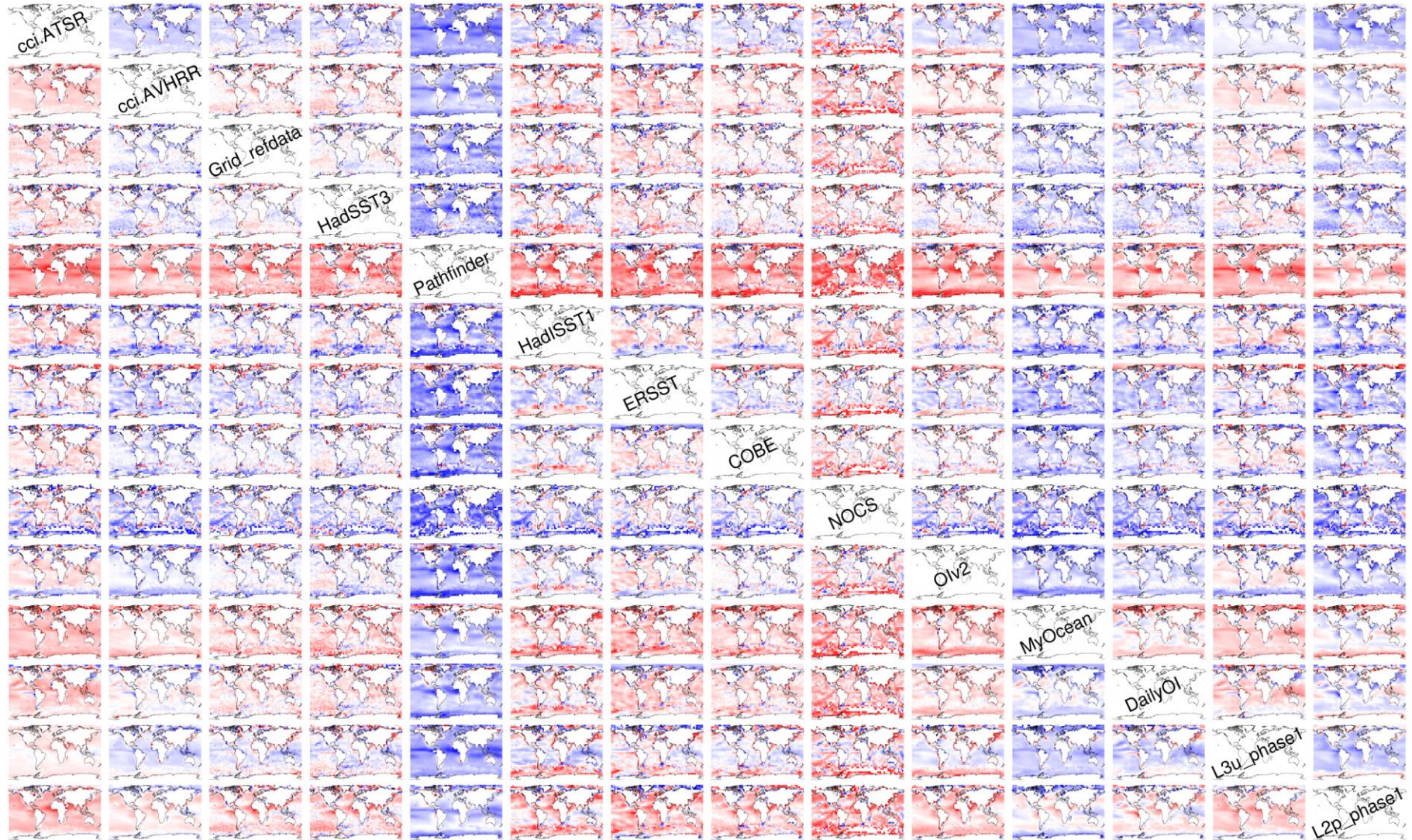
Figure 3-13. Colocated decadal (2001-2010) average differences between all pairs of data sets including precursor products from the Phase 1 SST CCI Release LT version 1.0. Colour scale is -1K to 1K (half the range of
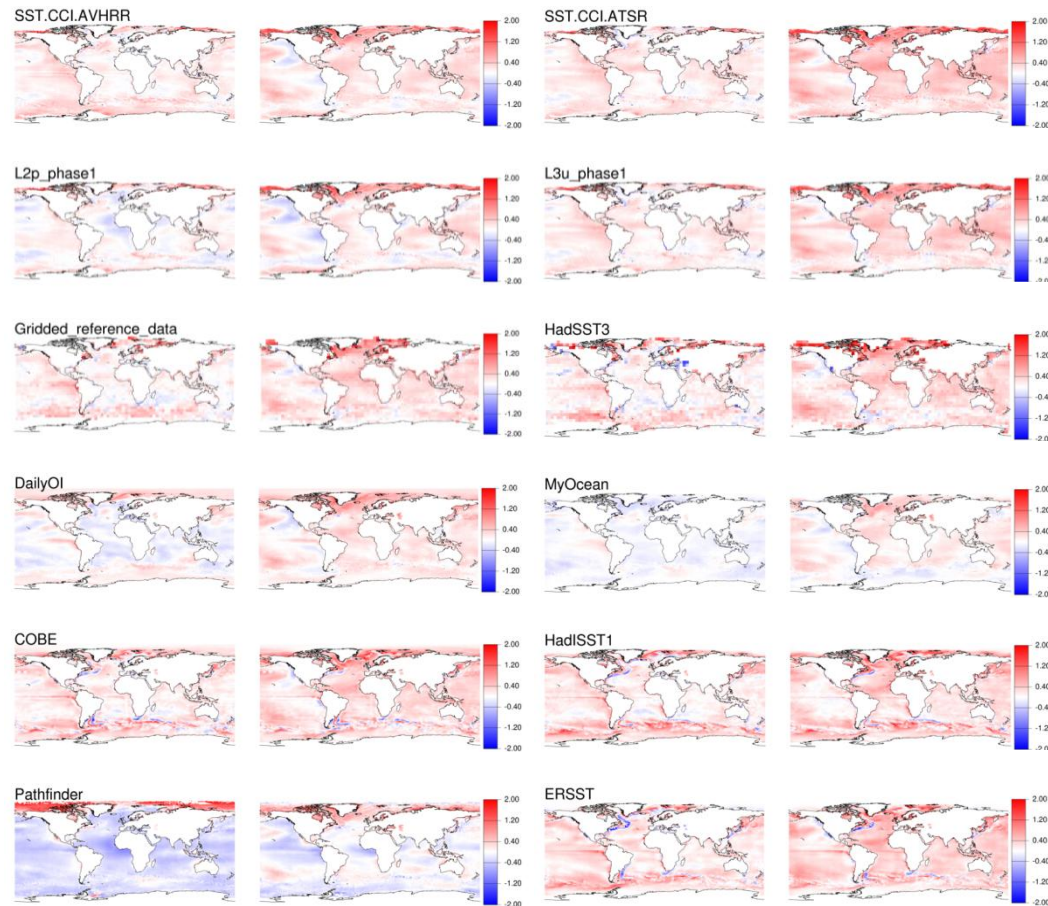

Figure 3-11). The difference is X minus Y, so for example the Pathfinder column is consistently negative because the Pathfinder data set has a cold bias relative to all the other data sets (i.e. Pathfinder minus other data set).

3.4.3   AUTO-CORRELATIONS

Auto-correlations for the SST CCI products are broadly comparable to those seen in other data sets, showing similar global patterns and a reduction in autocorrelations at greater lag (Figure 3-14). The global median autocorrelations for the SST CCI ATSR product are marginally higher than for the SST CCI AVHRR product, and both SST CCI products have marginally higher autocorrelations than their equivalent Phase 1 precursor at all lags.

The SST CCI ATSR product has higher global median autocorrelation than all the comparison datasets at all lags (with the exception of ERSST which has a marginally higher autocorrelation than SST CCI ATSR at 1-month lag, but lower autocorrelation at 2 to 4-month lags). The lowest autocorrelations are seen for the in situ only gridded products. For SST CCI ATSR, the reduction in the autocorrelation as the lag increases is smaller than for the comparison datasets and SST CCI AVHRR, with the exception of Pathfinder (which reduces at the same rate) and the gridded in situ datasets (which reduce at a smaller rate). The ERSST, HadISST1, COBE, MyOcean and DailyOI datasets display some negative correlations at high latitudes for lags greater than one month which may (partly) explain the greater reduction in autocorrelation as a function of lag seen for these datasets. The cause of these negative autocorrelations is not known but for these spatially complete products (and the climatology) it is likely related to the schemes used to infill sea surface temperatures in ice covered regions.

Although it is reassuring that all products show similar autocorrelation patterns, and that the SST CCI products do not show any stand out anomalous features relative to other datasets, it is difficult to judge which datasets are performing best as the true climatic autocorrelation fields are not known. In addition to autocorrelation due to true climatic variability, the datasets will suffer from biases which act to increase autocorrelation (by creating persistence in the sea surface temperatures) and random noise and sampling uncertainty which act to reduce the autocorrelation. It is difficult to say what combination of desirable and undesirable properties is causing the differences seen in autocorrelation seen between the datasets.
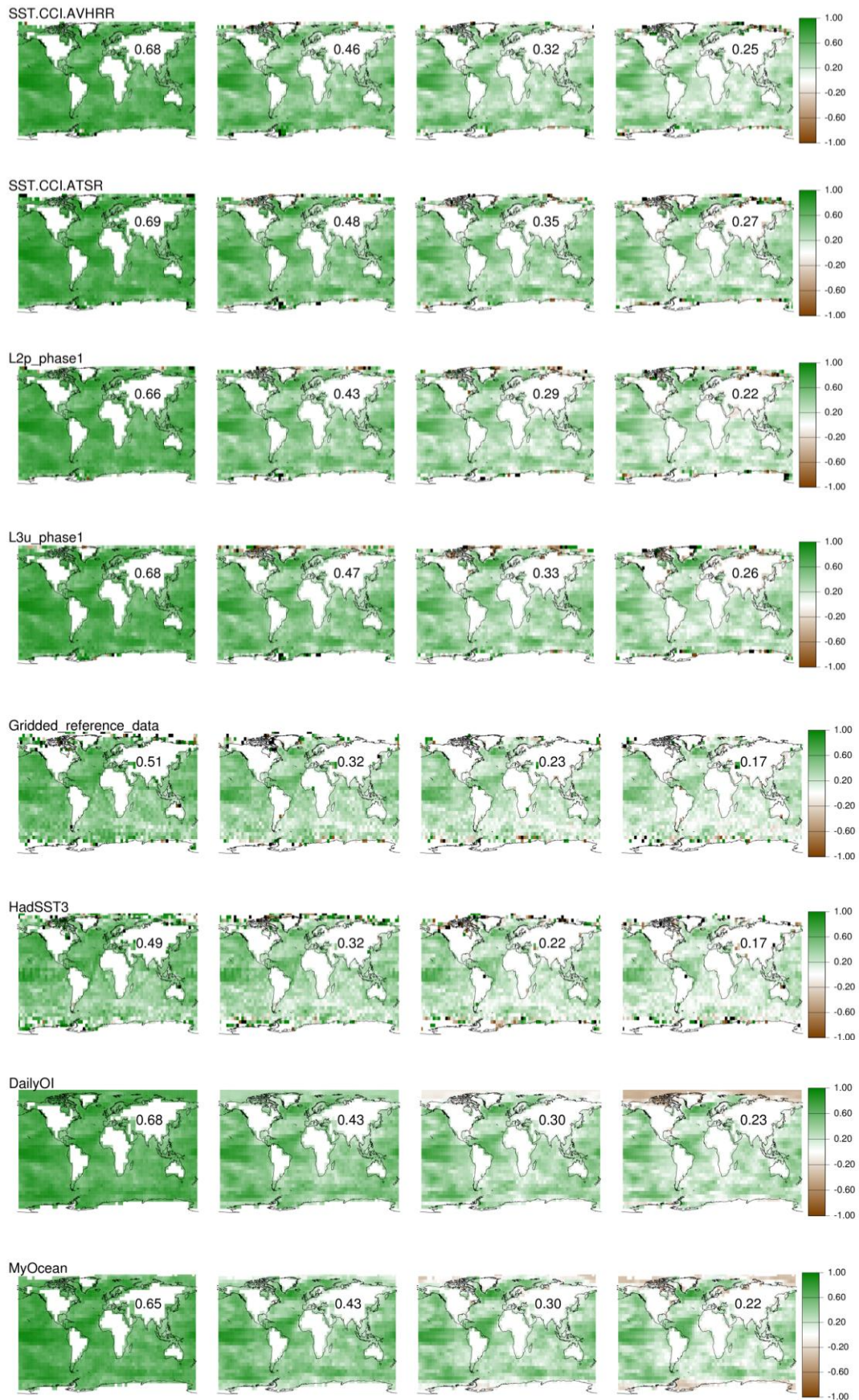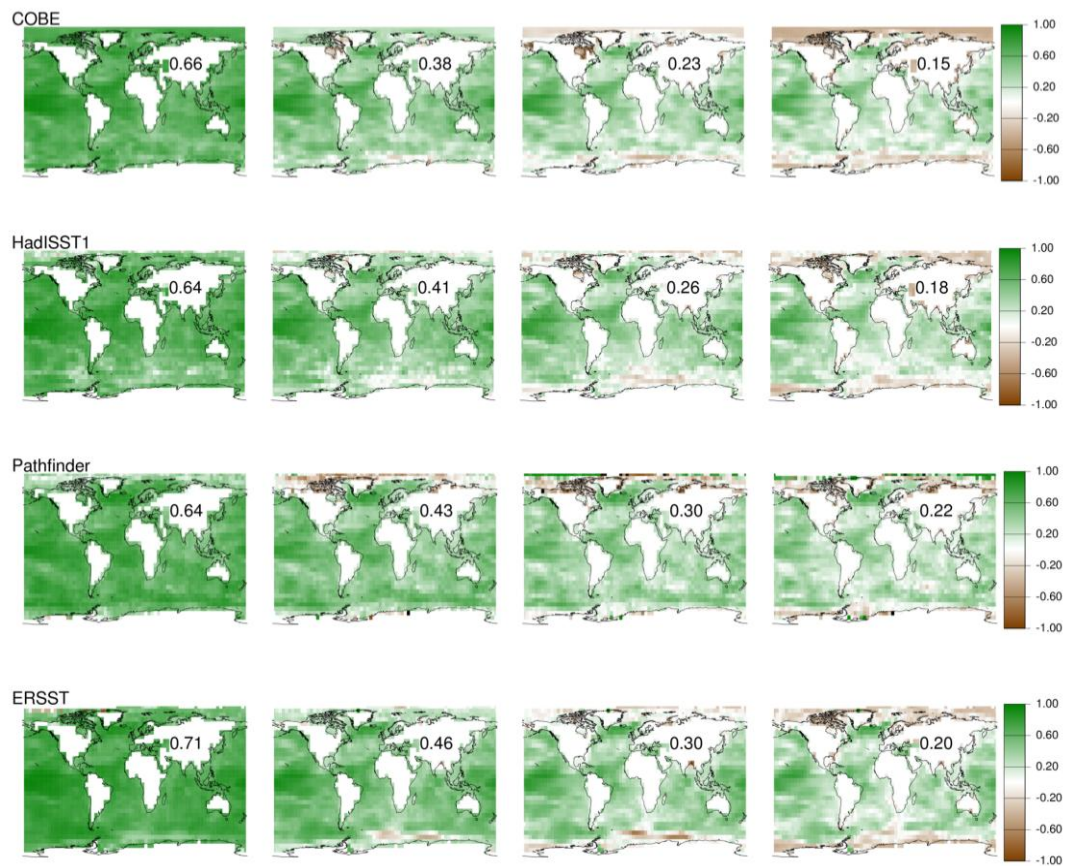
Figure 3-14. Lag correlations for lags from one to four months for a selection of datasets including precursor products from the Phase 1 SST CCI Release LT version 1.0. In each subplot, the number shown over central Asia is the global median lag correlation.

4. VOLUNTARY REPORTS BY REGISTERED USERS

4.1 Anne Stefaniak

European Space Agency

4.1.1 KEY MESSAGES

- The SST CCI data provides useful daily data providing high-resolution information for climate analysis. Using the CCI SST data product has been a focus of my research, comparing it with other data sets and using it to understand links between El Niño Southern Oscillation (ENSO) events in the central Pacific with variations in Arctic Sea Ice.

- Useful future developments could be to include the climatology / anomaly data as published in various CCI presentations to aid analysis and understanding of the data sets.

- The data is in an easy to use standard format, highly compatible with multiple programs and with other CCI projects aiding analysis of the data. However, when applying the sea ice mask (as provided with each SST daily file) to extract ocean temperatures only, an unexpected peak occurred in the first 3 months of 2008. This has since been attributed to an error in the sea ice mask and therefore the use of the mask was removed. As I understand there was some discussion about whether the data is to be reprocessed to fix this but it was not clear when this may happen.

- The tools to extract quick time-series data and subsets of regions would be very useful and should be made available as soon as possible for use with the data. Currently there appears to be no reported expected date for when these may be available.

4.1.1.1 AIMS OF THE STUDY

This research focuses on the effects of the El Niño Southern Oscillation (ENSO) events on Arctic Sea Ice using the ESA CCI data sets. Throughout this study both the ESA SST CCI Analysis long-term product version 1.0, satellite-only SST-depth analysis created by the OSTIA system from SST CCI ATSR and SST CCI AVHRR products, and the CCI Sea Ice data sets have been analysed and briefly compared with previously published data sets. The aim is to understand the links between ENSO events, originating in the Pacific, and variability in Arctic Sea Ice (concentration, extent and thickness). Various data analysis techniques are used to determine possible lag times for changes in the Pacific region to influence the Arctic. Further aims of this study are to understand the link between ENSO events and Arctic Sea Ice variability aiding prediction methods of Arctic Sea Ice in relation to the current 2014 / 2015 El Niño event.

4.1.1.2 METHOD

The SST CCI analysis data was downloaded from the ESA CCI link (ftp.ceda.ac.uk). The full time series of the SST CCI analysis covering 1991 – 2010 was analysed in R to extract the daily mean global SST. This method was also used to extract regional mean SST time series. Time series data was extracted initially by applying the sea ice mask, which highlighted the errors in 2008 and was then reprocessed without the mask. To aid interpretation of the data, the climatology files as described and provided by Claire Macintosh and Chris Merchant [University of Reading] were used to produce the daily global and regional anomalies. The daily global mean anomalies show an increasing trend throughout the SST CCI analysis time series. SST regional anomalies were extracted for the Niño regions (1+2, 3, 3.4 and 4), the Arctic Ocean and Greenland Sea.

Further analysis to understand the climate variability within the SST records used Principal Component Analysis (PCA) / Empirical Orthogonal Functions (EOF). This was

limited to annual SST anomaly means due to the volume of data and computer processor available.

4.1.1.3   RESULTS

Analysis of the global anomaly SST CCI analysis data shows a global increasing trend of +0.15 kelvin per decade (Figure 4-1). This overriding trend is attributed to warming SSTs in relation to climate change and has also been identified in various studies with longer data sets [Dyrrdal, 2008; RD.373]. ENSO events are clearly identified in comparison to the Southern Oceanic Index (SOI).
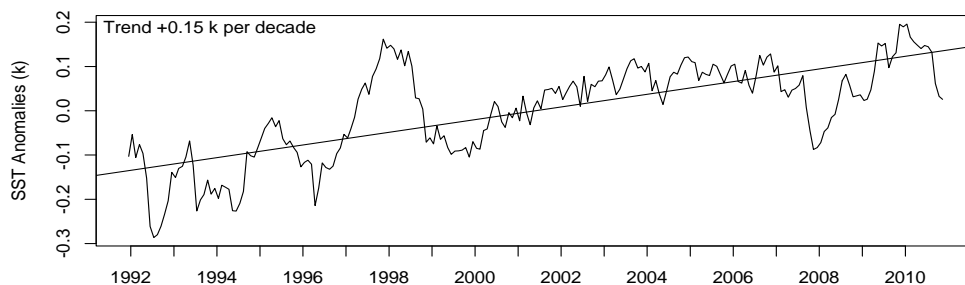

Figure 4-1. Global SST monthly anomalies calculated from the 1992–2010 climatology.

Regional time series highlights the ENSO events more clearly as shown in Figure 4-2 based on the Niño region 3.4. The red and blue lines indicate the ±0.5 K thresholds for ENSO events to be defined; however it is important to note that an ENSO event is defined by a 5 consecutive 3 month anomaly of ±0.5 K and therefore some of the shorter peaks and troughs did not advance into a full ENSO event, possibly due to a lack of the atmospheric coupling.
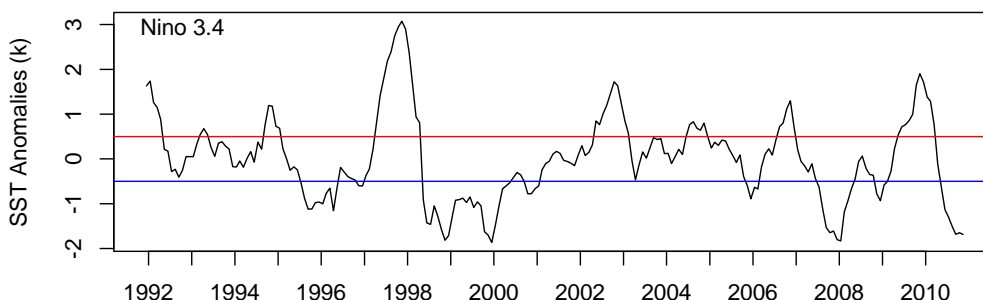

Figure 4-2. SST anomalies for the Niño 3.4 region; red line indicates the +0.5 K threshold for El Niño events and the blue line the -0.5 K threshold for La Niña events.

The hovmöller plot also shows how the 1997 -1998 El Niño dominates the ENSO events within the SST CCI analysis. Figure 4-3 indicates the anomalies for the Niño 3.4 region and also shows that over the last decade (2000 – 2010) the ENSO climate variability has largely been dominated by La Niña events.
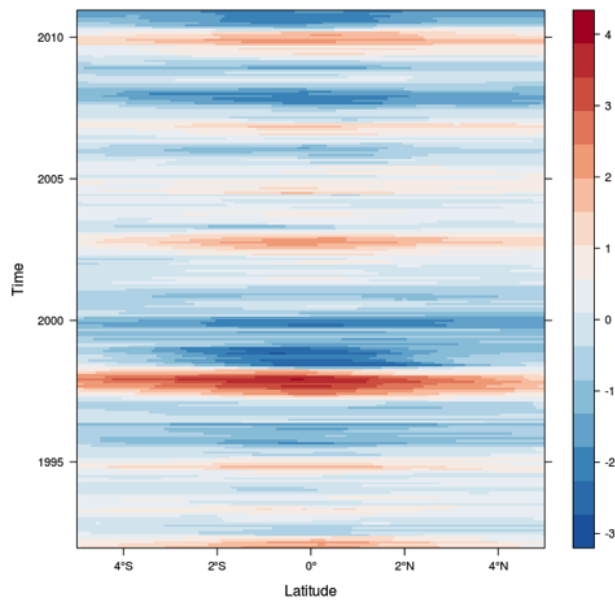
Figure 4-3. Hovmöller plot of the Niño 3.4 region highlighting the strong 1997 – 1998 El Niño event.

The PCA / EOF analysis of the SST CCI analysis anomaly data show the leading PCA accounted for approximately 26% of the variance and is attributed to ENSO, clearly depicting the spatial pattern of strong ENSO events (Figure 4-4). The second PCA is attributed to the North Pacific Mode and accounted for ~11%. Ideally this analysis would be processed using monthly SST anomalies and is being looked in to but initial results show expected patterns of climate variability within the SST CCI analysis data set.
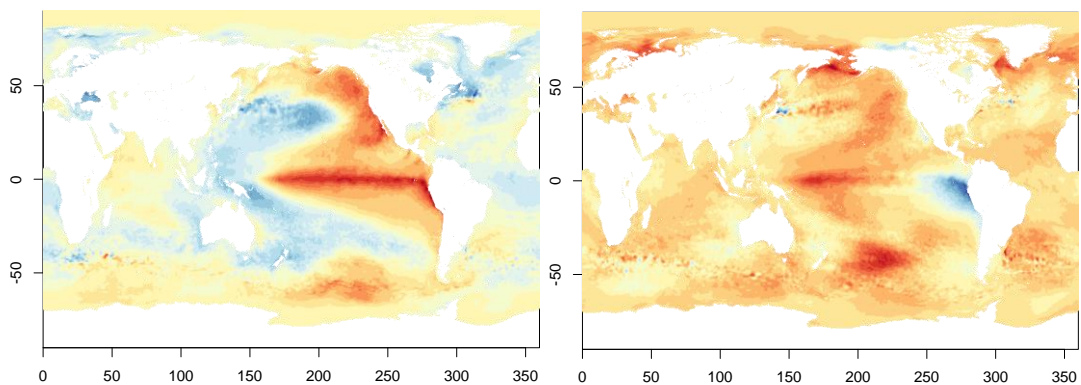
Figure 4-4. EOF analysis of the SST CCI analysis data showing the spatial patterns of the time series for the first two EOFs.

The spatial pattern of the leading EOF also shows very similar results to that discussed by Deser et al., 2010 [RD.374] highlighting positive SST anomalies within the eastern Pacific with negative SST anomalies to the west associated with ENSO events. Previous studies found similar albeit lower results for the leading EOF of SST anomalies associated with ENSO, including Deser et al., 2010 [RD.374] who accounted for 19% of the non-seasonal variability within the leading EOF.

Additional analysis techniques including cross-correlation of the Niño 3.4 region time series indicates the approximate periodicity of ENSO events in the data set is ~3.3 years; which fits within the 2-7 year ENSO cycle.

The SST CCI analysis data shows strong comparisons with other datasets regarding specific climatic events e.g. 1997/1998 El Niño event; however, the extent to which they vary differs to other datasets. Some initial comparisons with the Met Office Hadley Centre HadSST2 and HadSST3 [Rayner et al., 2006: RD.72; Kennedy et al., 2011b,c RD.210, RD.211] data sets were carried out which highlight the similarities in climate variability but at slightly different scales. The SST CCI Phase 1 Climate Assessment Report states that there are some discrepancies with comparison data especially pre-1995 due to instrument related biases, however, the SST CCI LT data is comparable to the comparison data sets in terms of their general evolution of SST and variability as found in the SST CCI Phase 1 CAR [RD.371, for further information].

4.1.1.4   CONCLUSIONS

The ESA SST CCI analysis data show clear evidence of multiple climate variability cycles influencing the time series including ENSO accounting for ~26% of the total variance. The data compare with additional data sets with some variation. Although further analysis is required, initial results are promising and exhibit many of the trends expected.

4.1.1.5   FEEDBACK ON SCIENTIFIC UTILITY OF THE SST CCI PRODUCTS

The results from this study largely corroborate previously published and analysed satellite data sets; however, some results vary when compared although indicating similar trends and patterns. The data files are easy to use and download from the website although it is slow.

5. FURTHER ISSUES AND RECOMMENDATIONS REPORTED BY REGISTERED USERS

5.1 Feedback on ease of use of the products and documentation

- The L4 data is presented in a standard, easy to access NetCDF data format with a good level of information in the Product User Guide to aid first time users. Some more information regarding the use of the mask would be useful and importance of applying the mask.

- Providing the anomaly data would be highly useful and cut down on many individual users processing time aiding multi-year comparisons.

- The newly added SST CCI Easy Download (http://www.esa-sst-cci.org/PUG/map.htm) is a great tool for first time users to start using and understanding the data.

5.2 Recommendations

- Reprocess the SST CCI analysis sea ice mask especially for 2008.

- Provide the climatology and/or the anomaly data files and information regarding how they have been calculated. For example with the sea level CCI data files both the absolute values and anomalies are available in separate variables within the daily NetCDF files.

- Longer time series of the data sets with more regular updates of recent data particularly with reference to the 2014/15 El Niño would provide highly useful data.

- The SST CCI Easy Download would be even more useful if you could highlight an area (i.e. draw a rectangle) to download data for a region rather than just one location.

This Page Is Intentionally Blank